



# Epigenetic Blockade of Hippocampal SOD2 Via DNMT3b-Mediated DNA Methylation: Implications in Mild Traumatic Brain Injury-Induced Persistent Oxidative Damage

Nagalakshmi Balasubramanian<sup>1</sup> · Sneha Sagarkar<sup>1,2</sup> · Amit G. Choudhary<sup>3</sup> · Dadasaheb M. Kokare<sup>3</sup> · Amul J. Sakharkar<sup>1</sup>

Received: 31 March 2020 / Accepted: 9 October 2020 / Published online: 25 October 2020  
© Springer Science+Business Media, LLC, part of Springer Nature 2020

## Abstract

The recurrent events of mild trauma exacerbate the vulnerability for post-traumatic stress disorder; however, the underlying molecular mechanisms are scarcely known. The repeated mild traumatic brain injury (rMTBI) perturbs redox homeostasis which is primarily managed by superoxide dismutase 2 (SOD2). The current study investigates the role of DNA methylation in SOD2 gene regulation and its involvement in rMTBI-induced persistent neuropathology inflicted by weight drop injury paradigm. The oxidative damage, neurodegenerative indicators, and SOD2 function and its regulation in the hippocampus were analyzed after 48 h and 30 days of rMTBI. The temporal and episodic increase in ROS levels (oxidative stress) heightened 8-hydroxyguanosine levels indicating oxidative damage after rMTBI that was concomitant with decline in SOD2 function. In parallel, occupancy of DNMT3b at SOD2 promoter was higher post 30 days of the first episode of rMTBI causing hypermethylation at SOD2 promoter. This epigenetic silencing of SOD2 promoter was sustained after the second episode of rMTBI causing permanent blockade in SOD2 response. The resultant oxidative stress further culminated into the increasing number of degenerating neurons. The treatment with 5-azacytidine, a pan DNMT inhibitor, normalized DNA methylation levels and revived SOD2 function after the second episode of rMTBI. The release of blockade in SOD2 expression by DNMT inhibition also normalized the post-traumatic oxidative consequences and relieved the neurodegeneration and deficits in learning and memory as measured by novel object recognition test. In conclusion, DNMT3b-mediated DNA methylation plays a critical role in SOD2 gene regulation in the hippocampus, and the perturbations therein post rMTBI are detrimental to redox homeostasis manifesting into neurological consequences.

**Keywords** Mild traumatic brain injury · DNA methylation · Superoxide dismutase 2 · Hippocampus · Neurodegeneration

## Introduction

Mild traumatic brain injury (MTBI) accounts to more than 80% of all the TBI [1]. The surge in incidences of repeated

MTBI (rMTBI) in recent years among sports [2, 3] and military personnel [4, 5] is concerning. The rMTBI exposure advances vulnerability to post-traumatic stress disorders [6–8] and chronic traumatic encephalopathy [9, 10] from subsequent injuries. Substantial evidences from the preclinical studies suggest the accumulative effect of repeated events of rMTBI in causing long-term behavioral impairments including depression [11], anxiety [12], and deficits in learning and memory [13–16]. Therefore, it is pertinent to investigate the neural substrates and molecular underpinnings of rMTBI-induced neuropathology.

The pathophysiology of TBI has been characterized by primary injury which further induces diffused long-lasting secondary injuries that result into exacerbated oxidative damage and progressive cell death [17]. Oxidative stress is one of the secondary injuries that begin at the time of the traumatic event and continue to contribute to cerebral damage for days

**Electronic supplementary material** The online version of this article (<https://doi.org/10.1007/s12035-020-02166-z>) contains supplementary material, which is available to authorized users.

✉ Amul J. Sakharkar  
amul.sakharkar@unipune.ac.in

<sup>1</sup> Department of Biotechnology, Savitribai Phule Pune University, Pune 411 007, India

<sup>2</sup> Department of Zoology, Savitribai Phule Pune University, Pune 411 007, India

<sup>3</sup> Department of Pharmaceutical Sciences, Rashtrasant Tukadoji Maharaj Nagpur University, Nagpur 440 033, India

and weeks following injury [18–20]. Endogenous antioxidant enzymes balance and control the oxidative stress. However, the extensive and rapid production of free radicals and reactive oxygen species (ROS) that occurs after the brain injury may prove devastating for the system [21]. Moreover, the TBI-induced glutamate excitotoxicity elevates the intracellular ROS levels [22] which are prevalently detoxified by mitochondrial manganese superoxide dismutase (MnSOD) or SOD2 [23, 24]. The hypofunction of this antioxidant enzyme manifests into neurodegeneration-associated disorders [25–29]. SOD2 heterozygous mice display alterations in the glutamatergic synaptic transmission in the hippocampus and cortex as well as impair spatial memory [25]. Interestingly, administration of SOD mimetic is known to improve age-associated memory deficits in mice [28].

Several rodent brain injury models such as fluid percussion, controlled cortical impact, blast, and weight drop (WD) are developed to investigate the consequences of rMTBI [30]. In particular, WD injury model induces non-penetrating diffused injury which simulates the rotational acceleration or deceleration of the brain during mishaps [31]. Using WD injury model, we have previously demonstrated the behavioral anomalies including memory deficits caused due to rMTBI [12, 13]. TBI induced by controlled cortical impact (CCI) injury in the SOD2 heterozygous mice reduces mitochondrial bioenergetics, while the mitochondrial function remained unaltered in the CCI-exposed SOD2-overexpressing mice [32]. Furthermore, the attenuated cellular SOD2 activity due to TBI results into oxidative stress which subsequently precipitates into secondary cellular damages in the brain [33]. On the contrary, Huber and colleagues have reported higher levels of SOD2 in the hippocampus of mice subjected to mild blast-induced trauma [34]. In the light of the above, the essentiality of understanding the upstream regulatory mechanisms of SOD2 gene regulation may not be undermined. The explication of such mechanisms will offer new clues about the TBI-induced neuropathological outcomes.

The modifications in the regulatory elements of the genes, collectively known as epigenetic changes, are known to maintain persistent alterations in the gene expression [35]. DNA methylation is the most stable, but reversible epigenetic mark which is regulated by the dynamic equilibrium in the activities of DNA methyltransferases (DNMT's) and demethylases [36]. We have previously shown that the rMTBI was able to alter the expression of DNMTs in the amygdala [12]. A plethora of studies have also reported trauma-induced persistent alterations in the active DNA methylation/demethylation on promoters of genes such as aralkylamine N-acetyltransferase, nitric oxide synthase 1 [37], and brain-derived neurotrophic factor (BDNF) [12]. It is therefore intriguing if such epigenetic mechanisms are operative in managing SOD2 dysfunction.

In the current study, we have investigated the potential role of DNA methylation in the SOD2 gene regulation and

implications of these mechanisms in long-term neuropathology due to rMTBI. Furthermore, the causality of DNA hypermethylation in the long-term disruption of SOD2 gene expression in the hippocampus was tested by treatment with 5-azacytidine (5-AzaC), a pan DNMT inhibitor, and by subjecting the rats to repeated episodes of rMTBI.

## Materials and Methods

### Animals

Adult male Wistar rats (200–225 g) were housed under controlled light (lights on 07:00–19:00 h) and temperature ( $25 \pm 2$  °C) conditions. Food and water were provided ad libitum. All the animal protocols in the present study were approved by Institutional Animal Ethics Committee (IAEC), Savitribai Phule Pune University, Pune and Department of Pharmaceutical Sciences, Rashtrasant Tukadoji Maharaj Nagpur University, Nagpur, India, and were performed as per the guidelines of National Institutes of Health (NIH), USA.

### Mild Traumatic Brain Injury

The rats were exposed to mild traumatic brain injury using the WD injury model as described previously [12, 13, 31]. Briefly, the instrument includes a hollow guide tube, clamp stand, and box. The rats were mildly anesthetized using diethyl ether and placed on the aluminum foil, which was attached firmly to the walls of the box. The uniform head impact was ensured by dropping a 200 g of metal weight with blunt end of 2 mm (length-6 cm, diameter-2 cm) from 30 cm height of hollow guide tube at the point of intersection of the diagonal lines that connects the eyes to the ears from contralateral sides.

**Experiment 1** The rats were exposed to either single MTBI or rMTBI with 3 or 5 hits on alternate days (Fig. 1a; Supplementary Fig. S1; Table 1). The experimental rats were divided into three groups based on the number of hits received, i.e., 1 hit (1M), 3 hits (3M), and 5 hits (5M). Further, each group was divided into two subgroups based on the sacrifice time, i.e., at 48 h and 30 days post trauma (1M-48h,  $n = 5$ ; 1M-30d,  $n = 5$ ; 3M-48h,  $n = 5$ ; 3M-30d,  $n = 5$ ; 5M-48 h,  $n = 5$ ; 5M—30d,  $n = 6$ ). All the animals were subjected to the MTBI procedure in parallel during 9 days of rMTBI episode. While the single MTBI (1M) was performed on the 1<sup>st</sup> day, the rMTBI with 3 hits (3M) was carried out by subjecting the rats to MTBI procedure on the 1<sup>st</sup> and 3<sup>rd</sup> day (Fig. 1a; Supplementary Fig. S1; Table 1). The respective sham controls (1M-SC,  $n = 5$ ; 3M-SC,  $n = 5$ ; 5M-SC,  $n = 5$ ) were subjected to the similar handling procedures, but did not receive weight drop

**Table 1** The details of sequential treatments received by rats in each group of different experiments. The number of mild traumatic brain injury/injuries (MTBI) is indicated by the number of hits during the first or both the episodes of repeated trauma paradigm

Group name	First episode	Drug/vehicle	Second episode
Experiment 1			
SC	Sham	--	--
1M	1 hit*	--	--
3M	3 hits*	--	--
5M	5 hits*	--	--
Experiment 2**			
SC-30d + V	Sham	Vehicle	--
SC-30d + A	Sham	5-AzaC	--
5M-30d + V	5 hits	Vehicle	--
5M-30d + A	5 hits	5-AzaC	--
Experiment 3***			
SC-30d + SC-48h	Sham	--	Sham
5M-30d + SC-48h	5 hits	--	Sham
SC-30d + 5 M-48h	Sham	--	5 hits
5M-30d + 5 M-48h	5 hits	--	5 hits
Experiment 4***			
SC-30d + V + SC-48h	Sham	Vehicle	Sham
SC-30d + A + SC-48h	Sham	5-AzaC	Sham
5M-30d + V + SC-48h	5 hits	Vehicle	Sham
5M-30d + A + SC-48h	5 hits	5-AzaC	Sham
5M-30d + V + 5 M-48h	5 hits	Vehicle	5 hits
5M-30d + A + 5 M-48h	5 hits	5-AzaC	5 hits

\*Animals were sacrificed at either 48 h or 30 days after the last event of trauma

\*\*Animals were sacrificed at 30 days after the last event of trauma

\*\*\*Animals were sacrificed 48 h after the second episode

injury and were sacrificed in parallel with respective groups. All the rats were decapitated under deep anesthesia using ketamine (60 mg/kg) and xylazine (10 mg/kg) solution injected intraperitoneally, and the brains were isolated for estimation of ROS and SOD2 mRNA levels. Two additional cohorts of 5 hits paradigm (SC, 5M-48h, 5M-30d) were generated and the brains were isolated for molecular (DNMT's mRNA levels; SOD2 protein levels, MeDIP-SEQ; MeDIP-qPCR; HMeDIP-qPCR; ChIP-qPCR) and biochemical (SOD2, catalase, and DNMT activities) analyses. One additional cohort of animals (SC,  $n = 5$ ; 5M-48h,  $n = 5$ ; 5M-30d,  $n = 5$ ) was perfused transcidentally for the isolation of the brains to perform histochemical analyses (SOD2 and 8-OHG immunofluorescence staining and FJC histochemical staining). Based on the observations of molecular, biochemical, and histochemical studies, we have employed rMTBI procedure with 5 hits for further experiments.

**Experiment 2** The rats subjected to the sham or rMTBI procedures were treated with 5-AzaC to study the effects of DNMT

inhibition on the rMTBI-induced molecular and behavioral changes (Fig. 1b; Table 1). As described previously [12], 5-AzaC (2 mg/kg) or equivalent volumes of vehicle were injected intraperitoneally for 3 consecutive days (each injection 24 h apart on the 28<sup>th</sup>, 29<sup>th</sup>, and 30<sup>th</sup> day post trauma). The SC- and rMTBI-induced animals were divided into two subgroups each. While one subgroup was treated with 5-AzaC (SC-30d + A,  $n = 5$  and 5M-30d + A,  $n = 6$ ), another subgroup was treated with vehicle (SC-30d + V,  $n = 5$  and 5M-30d + V,  $n = 6$ ). After 2 h of the vehicle or 5-AzaC treatment, the animals were subjected to measurements of learning and memory behaviors using novel object recognition (NOR) test. Immediately, after the behavior testing, the rats were decapitated under anesthesia to isolate the brains for molecular (SOD2 mRNA, protein levels; MeDIP-qPCR; HMeDIP-qPCR) and biochemical (SOD2 activity and ROS levels) analyses. An additional cohort of animals (SC-30d + V,  $n = 5$ ; 5M-30d + V,  $n = 5$ ; SC-30d + A,  $n = 5$  and 5M-30d + A,  $n = 5$ ) was subjected to the similar treatments as described above, and the animals were transcidentally perfused for the isolation of the brain to perform

histochemical analyses (8-OHG immunofluorescence and FJC staining).

**Experiment 3** The sham- or rMTBI-exposed rats were subjected for an additional episode of either sham or rMTBI procedures to study the effects of two episodes of rMTBI on SOD2 regulation and function. The second episode of rMTBI with 5 hits was performed after 30 days of the first episode (Fig. 1c; Table 1). The rMTBI-induced rats with single episode were divided into two groups; one group was exposed to the 2<sup>nd</sup> episode of rMTBI (5M-30d + 5M-48h,  $n = 6$ ), and the other group was subjected to sham procedure (5M-30d + SC-48h,  $n = 5$ ). In parallel, the first episode sham-exposed rats were also divided into two groups; one group was subjected to the 2<sup>nd</sup> episode of rMTBI (SC-30d + 5M-48h,  $n = 5$ ), and the other group was exposed to the 2<sup>nd</sup> episode of sham procedure (SC-30d + SC-48h,  $n = 5$ ) after 30 days of the first episode and served as controls. All the rats in these groups were sacrificed post 48 h of the 2<sup>nd</sup> episode and the brains were collected for

further molecular (SOD2 and DNMTs mRNA levels; SOD2 protein) and biochemical (ROS levels, SOD2 activity) analyses. An additional cohort of three groups of animals (SC-30d + SC-48h,  $n = 5$ ; 5M-30d + SC-48h,  $n = 6$ ; 5M-30d + 5M-48h,  $n = 6$ ) was generated for the analysis of epigenetic changes (MeDIP-qPCR and ChIP-qPCR) during the 2<sup>nd</sup> episode. In addition, yet another cohort of three groups of animals (SC-30d + SC-48h,  $n = 5$ ; 5M-30d + SC-48h,  $n = 5$ ; 5M-30d + 5M-48h,  $n = 5$ ) was perfused transcardially and the brains were isolated to perform histochemical analyses (8-OHG immunofluorescence staining and FJC histochemical staining).

**Experiment 4** The 5-AzaC was administered to the animals subjected to one or two episodes of rMTBI procedures before the second episode to examine the effect of DNMT inhibition on SOD2 response after second episode (Fig. 1d, Table 1). The animals exposed to the 1<sup>st</sup> episode of rMTBI (5M) were divided into two subgroups. One of them was exposed to the

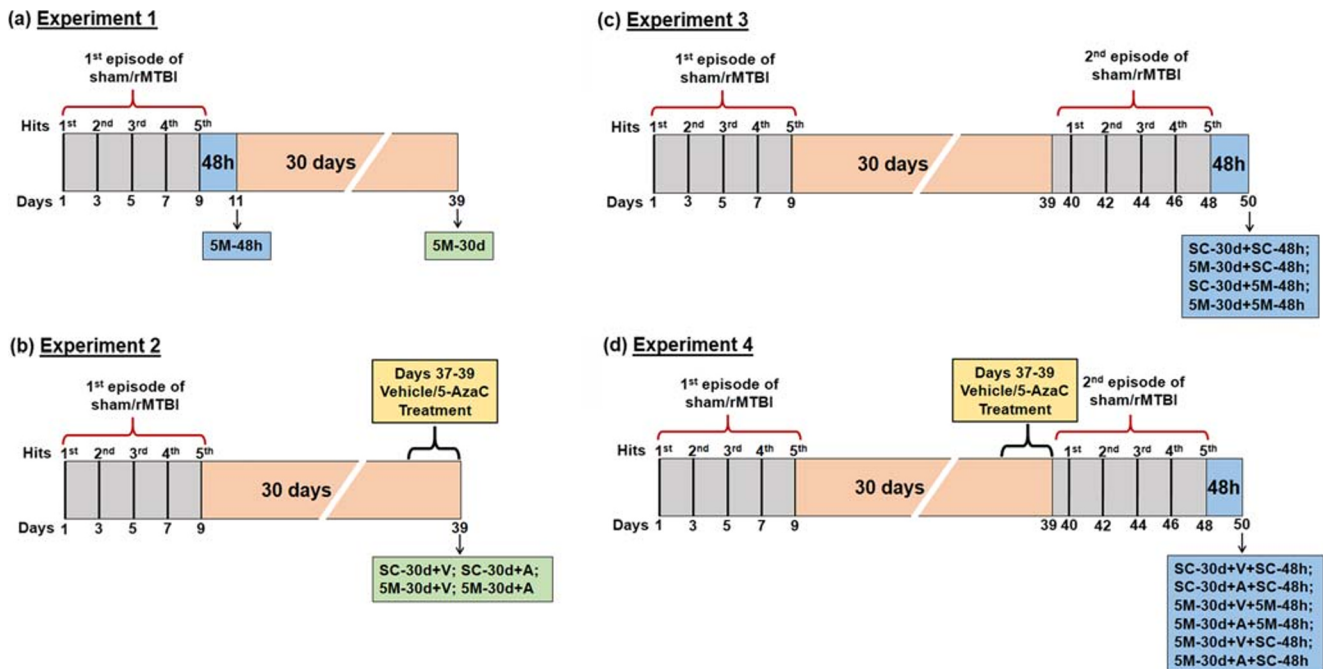


**Fig. 1** Experimental paradigm. **a** The rats were subjected to rMTBI (5 hits on alternate days) and sacrificed either at 48 h (5M-48h,  $n = 5$ ) or 30 days (5M-30d,  $n = 6$ ). The sham controls (SC,  $n = 5$ ) were also generated at both the time points. Two additional cohorts of groups of animals subjected to similar experiment were generated for molecular and biochemical analyses. Additional cohort of animals (SC,  $n = 5$ ; 5M-48h,  $n = 5$ ; 5M-30d,  $n = 5$ ) was perfused transcardially and the brains were used for histochemical studies. **b** To investigate the role of DNA methylation on rMTBI-induced persistent alterations, the rMTBI- or sham-exposed rats were either treated with vehicle (V) or 5-AzaC (A) on the 37<sup>th</sup>, 38<sup>th</sup>, and 39<sup>th</sup> day and sacrificed after 2 h of the last treatment (SC-30d + V,  $n = 5$ ; SC-30d + A,  $n = 5$ ; 5M-30d + V,  $n = 6$ ; 5M-30d + A,  $n = 6$ ). Additional cohort of animals (SC-30d + V,  $n = 5$ ; SC-30d + A,  $n = 5$ ; 5M-30d + V,  $n = 5$ ; 5M-30d + A,  $n = 5$ ) was generated for histochemical studies. **c** To study the acute response of SOD2 to the repeated

episodes of rMTBI, two episodes of 5 hits each were given to the rats. The second episode of rMTBI or sham procedures was given after 30 days of the first episode (5M-30d + SC-48h,  $n = 5$ ; SC-30d + 5M-48h,  $n = 5$ ; 5M-30d + 5M-48h,  $n = 6$ ). Double sham control rats were also generated (SC-30d + SC-48h,  $n = 5$ ) in parallel. All the rats were sacrificed after 48 h of the second episode. Additional cohort of animals (SC-30d + SC-48h,  $n = 5$ ; 5M-30d + SC-48h,  $n = 5$ ; 5M-30d + 5M-48h,  $n = 5$ ) was generated for histochemical studies. **d** The rats subjected to double episodic rMTBI paradigm were either treated with vehicle (V) or 5-AzaC (A) before the 2<sup>nd</sup> episode (5M-30d + V + SC-48h,  $n = 5$ ; 5M-30d + A + SC-48h,  $n = 5$ ; 5M-30d + V + 5M-48h,  $n = 5$ ; 5M-30d + A + 5M-48h,  $n = 5$ ). Sham control rats were also generated on concurrent days as that of rMTBI (SC-30d + V + SC-48h,  $n = 5$ ; SC-30d + A + SC-48h,  $n = 5$ ). rMTBI, repeated mild traumatic brain injury; 5-AzaC, 5-azacytidine

2<sup>nd</sup> episode of rMTBI (5M) and the other was subjected to sham procedures. These groups were further subdivided into two groups based on the administration of 5-AzaC (5M-30d + A + SC-48h,  $n = 5$ ; 5M-30d + A + 5M-48h,  $n = 5$ ) and vehicle (5M-30d + V + SC-48h,  $n = 5$ ; 5M-30d + V + 5M-48h,  $n = 5$ ). In addition, the animals which received sham procedures during both the episodes were also treated with either 5-AzaC (SC-30d + A + SC-48h,  $n = 5$ ) or vehicle (SC-30d + V + SC-48h,  $n = 5$ ) after 30 days of the 1<sup>st</sup> episode of sham procedures. All the animals were euthanized after 48 h of the 2<sup>nd</sup> episode and the brains were collected for further molecular (SOD2 mRNA and protein levels; MeDIP-qPCR) and biochemical (SOD2 activity) analyses.

## Cell Culture

The PC12 cell line was obtained as a generous gift from Dr. Chaitanya Athale (Indian Institute of Science Education and Research, IISER-Pune, India). The cells were cultured at 37 °C in an atmosphere of 5% CO<sub>2</sub> and 95% air in Opti-MEM media (ThermoFisher Scientific, USA). The Opti-MEM was supplemented with 5% (*v/v*) fetal bovine serum (FBS; 10270106, Gibco® Life Technologies, CA, USA), 10% (*v/v*) of heat-inactivated horse serum (Sigma, MO, USA), 100 U/mL penicillin, and 100 µg/mL streptomycin. The PC12 cells were differentiated into neuron-like cells by treating in a differentiation medium (Opti-MEM containing 0.5%, *v/v*, FBS; 100 U/mL penicillin; 100 µg/mL streptomycin; 50 ng/ml of nerve growth factor; 13257019, ThermoFisher Scientific, USA) for 9 days. Sub-lethal dose of glutamate was used to mimic the oxidative damage observed in rMTBI. As previously examined [38], the cells were exposed to 15 mM glutamate for 24 h. For silencing DNMT3b, the glutamate-treated PC12 cells were transfected with DNMT3b siRNA (Eurogentec, Belgium) using Lipofectamine® MessengerMAX Transfection Reagent (ThermoFisher Scientific, USA) according to manufacturer's instructions. Furthermore, the cells were collected by scraping and used for molecular analyses (SOD2 and DNMT3b mRNA levels; MeDIP-qPCR).

## Novel Object Recognition Test

The effect of 5-AzaC on the recognition memory of rMTBI-induced rats was studied using NOR test as described previously [13]. Briefly, the NOR test includes three phases: habituation, acquisition, and test session. Habituation for NOR procedure was carried out on the 37<sup>th</sup> day (28<sup>th</sup> day post rMTBI). The rat was allowed to habituate the open field for 10 min without any object. After 24 h of habituation phase, on the 38<sup>th</sup> day (29<sup>th</sup> day post rMTBI), the rat was subjected to acquisition trial for 5 min, where it was allowed to explore the two identical objects. Furthermore, the rats were subjected to

the testing phase after 24 h, i.e., on the 39<sup>th</sup> day (30<sup>th</sup> day post rMTBI), when one of the objects was replaced with novel object. The 5-AzaC was administered 2 h before the habituation, acquisition, and testing phases on the 37<sup>th</sup>–39<sup>th</sup> day (28<sup>th</sup>–30<sup>th</sup> day post rMTBI) respectively. The exploration time was measured by the observer blind to the treatments. The exploration behavior of the rats was defined by the typical behavior such as sniffing or poking the object with the nose. The exploration time for each object was recorded to measure discrimination index (DI). The DI represents the proportion of time spent for exploring both the familiar (F) and novel (N) objects in the testing phase [13, 39, 40]. The formula for calculating DI is  $N-F/N + F$  ( $N$  = time spent with novel object and  $F$  = time spent with familiar object). The positive score of DI indicates preference to the novel object while negative score correlates to the preference for the familiar object [41–43]. The discrimination of novel object over familiar object during the test session indicates the impairment in the recognition memory.

## ROS Detection by H2DCFDA Dye

The intracellular change in ROS levels was detected by using 2', 7'-dichlorodihydrofluorescein diacetate dye (H2DCFDA; ThermoFisher Scientific, USA). As previously described [44], the tissue was homogenized in ROS buffer and incubated with H2DCFDA dye. The reaction was stopped with 70% ethanol, 0.1 N HCl, and neutralized by 1 M NaHCO<sub>3</sub>. The ROS levels were then evaluated by measuring fluorescence intensity with excitation at optical density (OD) of 485 nm and emission at OD 535 nm in a multimode microplate reader (Hidex, Germany). Intensity of fluorescence was expressed as relative fluorescence units (RFU).

## Reverse Transcriptase-Quantitative PCR (RT-qPCR) for mRNA Measurements

Total RNA was isolated using TRIZOL reagent (Ambion, USA) as described previously [12, 13, 45]. The DNA contamination was eliminated using DNA-free™ DNA Removal Kit (Life Technologies, USA). The RNA was checked for its purity and quantified using Biospec Nano spectrophotometer (Shimadzu, Japan). The reverse transcription was performed using iScript cDNA synthesis kit (Bio-Rad Laboratories, CA, USA). The thermal profile used for the reverse transcription was 25 °C for 5 min, 45 °C for 20 min, and 95 °C for 1 min. Quantitative reverse transcription PCR (RT-qPCR) for the target gene (GAPDH, SOD2, DNMT1, DNMT3a, DNMT3b) was performed using SYBR green qPCR master mix (Bio-Rad Laboratories, USA) on CFX96™ Real-time-PCR System (Bio-Rad Laboratories, Singapore). Specific primer sets used for amplification of target cDNA are mentioned in Table 2. The data were analyzed using GAPDH as an

**Table 2** List of primers used for mRNA expression analysis using RT-qPCR

Gene name	Forward/reverse (5'-3')	Sequence
GAPDH	Forward	ATGACTCTACCCACGGCAAG
	Reverse	CTGGAAGATGGTGATGGGTT
DNMT1	Forward	AAGCCAGCTATGCGACTTGAAAC
	Reverse	ACAACCGTTGGCTTCTGAGTGAG
DNMT3a	Forward	CACCTACAACAAGCAGCCCATGTA
	Reverse	AGCCTTGCCAGTGTCACTTTCATC
DNMT3b	Forward	TGTGCAGAGTCCATTGCTGTAGGA
	Reverse	GCTTCCGCCAATCACCAAGTCAAA
SOD2	Forward	GTGTCTGTGGGAGTCCAAGG
	Reverse	TGCTCCCACACATCAATCCC

internal control. We have previously reported the GAPDH as the best housekeeping gene for the gene expression analysis employing rMTBI model [46]. The cycling parameters used for real-time PCR were as follows: 95 °C for 10 min followed by 40 cycles of 95 °C for 15 s, 60 °C for 15 s. After the PCR amplification, melt curves for the products were generated by heating at the temperature range from 60 to 95 °C in 0.5 °C increments at a rate of 5 s/step. Fold changes in the mRNA levels were determined for each gene after normalization to GAPDH using  $2^{-\Delta\Delta CT}$  method [47]. Results are represented as fold changes in the mRNA levels ( $\pm$  SEM).

### Western Blot

Total protein from hippocampal tissue was isolated using RIPA lysis buffer. To check the subcellular localization of SOD2, the mitochondrial fraction was separated using mitochondrial isolation kit (ThermoFisher Scientific, USA), according to the manufacturer's instructions and lysed using Tris buffer containing 2% CHAPS. The proteins were quantified using BCA method (ThermoFisher Scientific, USA) and resolved by SDS-PAGE in a 12% polyacrylamide gel. The resolved proteins were further transferred to PVDF membrane (0.45  $\mu$ m; Millipore, USA) for immunoblotting according to standard procedures. The blots were blocked using Starting Block T20 (TBS) Blocking Buffer (ThermoFisher Scientific, USA) and incubated 16 h with antibodies. We used the following antibody dilutions: 1:500 for rabbit polyclonal antibody against MnSOD (06–984, Millipore, USA); 1:2000 for rabbit polyclonal antibody against HSP60 (E-AB-70103, Elabscience, USA); and 1:5000 for rabbit polyclonal antibody against  $\beta$ -actin (ab8227, Abcam, UK). A dilution of 1:5000 of HRP conjugate secondary antibody (Thermo scientific, USA) was used to detect the primary antibodies. Enhanced chemiluminescent reagent (ECL; Advansta, USA) was applied on the blot and images were acquired using My ECL Imager (Chemi-Doc, Thermo Scientific, USA). Protein bands were quantified using Image J 1.45 software (National Institutes of Health, Bethesda, MD). Average relative density of the

proteins was determined after normalization to  $\beta$ -actin (total protein) or HSP60 (mitochondrial protein). Results are represented as average relative density of the protein levels ( $\pm$  SEM).

### SOD2 Activity

The SOD2 activity in the hippocampus was measured using SOD activity assay kit as per manufacturer's instructions (K335, BioVision, CA, USA). Briefly, the hippocampal tissue was homogenized in ice cold 0.1 M Tris-HCl (pH 7.4) containing 0.5% Triton X-100, 5 mM  $\beta$ -ME, and 0.1 mg/ml PMSF. The homogenate was spun at 14000g for 5 min at 4 °C and the supernatant was treated with 2 mM potassium cyanide (KCN) to inhibit SOD1 activity. WST-1 produces a water-soluble formazan dye upon reduction with superoxide anion which was measured colorimetrically at OD 450 nm by a multimode microplate reader (Hidex, Germany). Results are represented as percentage activity of control ( $\pm$  SEM).

### Catalase Activity

The catalase activity in the hippocampus was measured using a catalase activity assay kit as per the manufacturer's instructions (ab83464, Abcam, USA). Briefly, hippocampal tissue (25 mg) was homogenized in ice-cold assay buffer. The homogenate was centrifuged at 10000g for 15 min at 4 °C and supernatant was treated with freshly prepared 1 mM  $H_2O_2$ . In the absence of catalase, the  $H_2O_2$  gets accumulated in the cell which reacts with OxiRed probe to produce a product that can be detected fluorometrically at Ex/Em = 535/587 nm in a multimode microplate reader (Hidex, Germany). Results are represented as nmol/min/ml activity as compared to controls ( $\pm$  SEM).

### DNMT Activity

The nuclear protein fraction of the hippocampus was isolated using CellLytic™ NuCLEAR™ Extraction Kit (NXTRACT;

Sigma, USA). The DNMT activity in the nuclear protein fraction (20  $\mu$ g) was estimated using EpiQuik™ DNA methyltransferases activity/inhibition assay kit (Epigentek, Brooklyn, NY, USA) as reported previously [12]. Multimode microplate reader (Hidex, Germany) was used to record the OD at 450 nm and the results are represented as percentage of control ( $\pm$  SEM).

### Methylated and Hydroxymethylated DNA Immunoprecipitation Assay

The methylated (MeDIP) and hydroxymethylated DNA immunoprecipitation (HMeDIP) assay was performed to examine the levels of 5-methylcytosine (5mc) and 5-hydroxymethylcytosine (5hmc) at the SOD2 promoter, as previously reported [12]. In brief, the DNA was isolated from the hippocampal tissue by phenol-chloroform method (Invitrogen, USA). The purified DNA was sonicated in a water-bath sonicator to produce 200–500 bp fragments. The DNA was further heat denatured and used for immunoprecipitation using the antibodies against 5mc (A-3001, Zymo, USA) or 5hmc (C15310210, Diagenode, Belgium) for overnight at 4 °C. A fraction of sonicated DNA was separately stored for further use as input DNA. The antibody-DNA complex was incubated with protein A/G PLUS-agarose™ beads (Santa Cruz Biotechnology, USA) for 2 h. The bead-antibody-DNA complex was serially washed through low salt, high salt, and Tris-EDTA buffers. The DNA was eluted from the beads in the elution buffer at 67 °C. The eluted DNA was cleaned by using phenol-chloroform method. The qPCR was performed to amplify the immunoprecipitated and input DNA using the SYBR Green qPCR Master Mix (Bio-Rad Laboratories, USA) and primers specific to SOD2 promoter (Forward: 5'-GTCTGAGGGTGGAGCATAGC-3', Reverse: 5'-CTGCTCTCCTCAGAACACGG-3'). The input DNA was used in parallel as the internal control to normalize the Ct values of the immunoprecipitated DNA. The normalized Ct values were used to calculate the fold changes in the methylation and hydroxymethylation levels using  $2^{-\Delta\Delta CT}$  method [47]. The results are represented as mean fold changes ( $\pm$  SEM) with respect to controls.

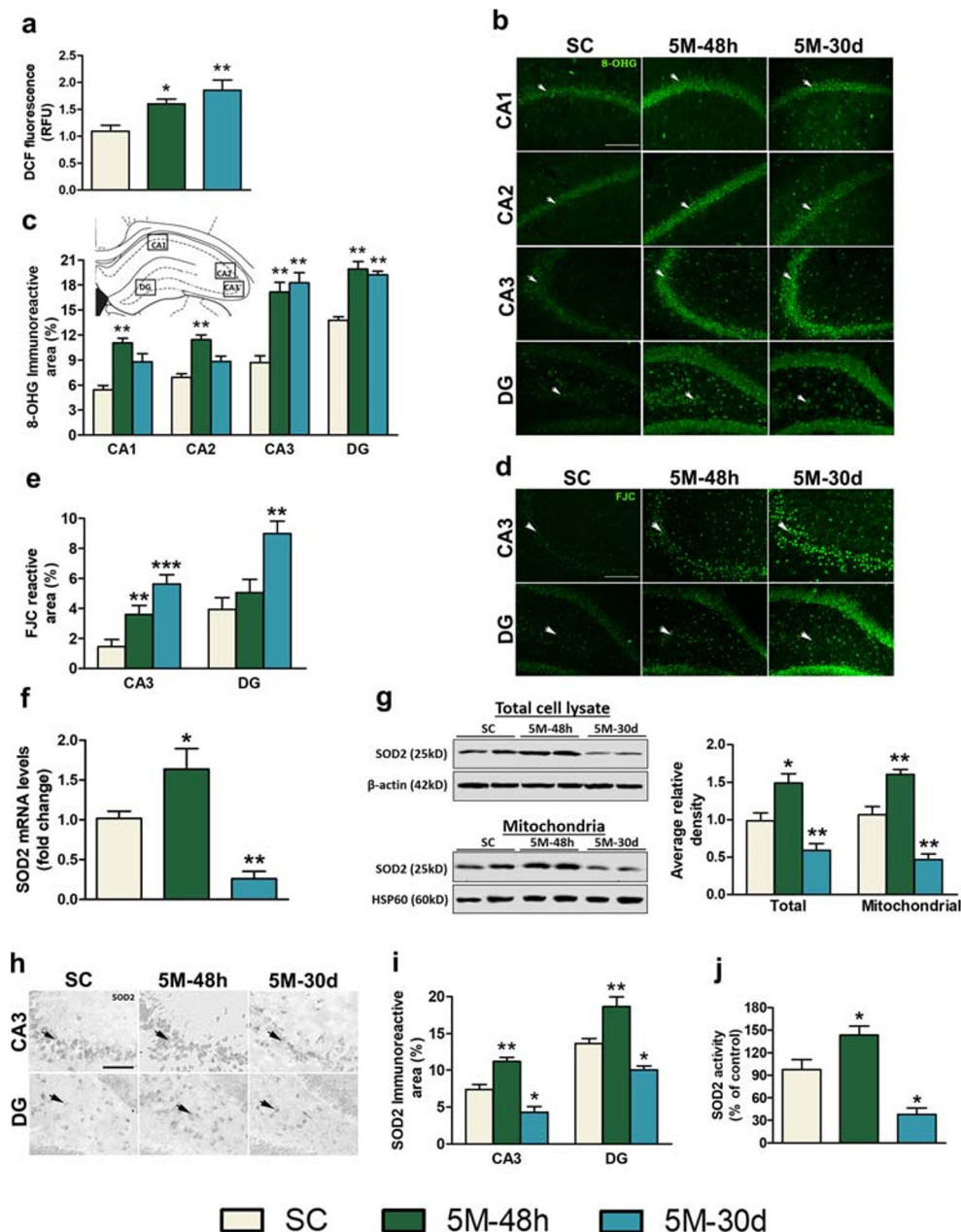
### Methylated DNA Immunoprecipitation Sequencing and Analysis

The MeDIP sequencing was performed on the Illumina platform (Eurofins India Pvt. Ltd., Bangalore, India). DNA was isolated from the hippocampus using CTAB phenol-chloroform method followed by RNase A treatment. Quality and quantity of DNA were checked by nanodrop spectrophotometer (ThermoFisher Scientific, USA). The DNA was fragmented using ultrasonicator (Covaris M220,

ThermoFisher Scientific, USA) to generate a mean fragment distribution of 150 bp and these fragments were further subjected to end-repair. MagMeDIP kit was used for the immunoprecipitation of the methylated DNA. Paired-end Illumina libraries were prepared using TruSeq Nano DNA library prep kit (Illumina, USA), as per the manufacturer's instructions and evaluated for size distribution and concentration using an automated electrophoresis system (4200 Tape station system, Agilent technologies). The libraries were then loaded on NextSeq 500 for cluster generation and sequencing which generated paired-end reads of 90–100 nucleotides. The results were analyzed for data quality and adaptor trimming using Trimmomatic (v0.35). The high-quality reads were mapped to the rat genome (*Rattus norvegicus*) v6.0 using the BWA-Mem with default parameter. Furthermore, alignment files were processed by Samtools to convert the alignment output into BAM files and the BED files were generated by MACS2 peak caller. Differential methylation profiles of SOD2 and GAPDH genes were visualized using Integrative Genomics Viewer (IGV) version 2.5.0 [48].

### Chromatin Immunoprecipitation Assay

Chromatin immunoprecipitation (ChIP) was performed to measure DNMT3b occupancy at the SOD2 promoter as described previously [13]. In brief, the tissue was homogenized with cold PBS and fixed in 4% formaldehyde at 37 °C for 10 min. The fixation reaction was quenched by adding glycine. The homogenate was centrifuged at 1200g for 10 min; the pellet was resuspended in SDS-lysis buffer and sonicated to shear the chromatin. Sheared chromatin (200  $\mu$ l) was immunoprecipitated using antibody against DNMT3b (2  $\mu$ g; sc-376043, Santacruz, USA) at 4 °C overnight. A part of sheared chromatin was separated to use as input. The chromatin-antibody complex was incubated with protein A/G PLUS-agarose™ beads (Santa Cruz Biotechnology, USA) for 4 h at 4 °C. The beads-antibody-chromatin complex was serially washed through low salt, high salt, and Tris-EDTA buffers. The chromatin was eluted in elution buffer by incubating the complex at 67 °C for 2 h. Both the input and immunoprecipitated chromatin were subjected to proteinase K digestion for 2 h at 55 °C and DNA was isolated by the phenol-chloroform method. Quantitative PCR was performed to amplify the immunoprecipitated and input DNA using the SYBR Green qPCR Master Mix (Bio-Rad Laboratories, USA) and the primers specific to SOD2 promoter as given in the “[Methylated and Hydroxymethylated DNA Immunoprecipitation Assay](#)” section. Fold changes were calculated after normalizing the Ct values of immunoprecipitated DNA to input DNA using  $2^{-\Delta\Delta CT}$  method [46]. The results are represented as mean fold changes ( $\pm$  SEM) with respect to sham controls.



## Immunohistochemistry

The immunohistochemistry was performed for the localization of the SOD2 and 8-hydroxyguanosine (8-OHG) in the hippocampus, as reported previously [13, 45]. Briefly, the animals were perfused transcardially using normal saline followed with 4% paraformaldehyde (PFA). The animals were decapitated after the perfusion and the brains were kept in 4% PFA overnight for post fixation. The fixed brains were transferred serially to 15% and 30% sucrose solutions and were cut on cryomicrotome (Leica Microsystems, Germany) at 20  $\mu$ m thickness. The sections were washed in 0.01 M PBS and blocked in 1% BSA in PBST for 30 min. The sections

were incubated with mouse monoclonal antibodies against 8-OHG (ab62623, Abcam, UK) at 1:2000 dilution. After incubation, the sections were washed with PBS and incubated with secondary antibodies anti-mouse IgG-Alexa fluor 488 (A11001, ThermoFisher Scientific, USA) at 1:500 dilution for the detection of immunoreactivity. The sections were washed with PBS, mounted on slides with mounting medium (Vectashield, Vector Laboratories, CA, USA), and observed under the epifluorescence microscope (DM-4500, Leica Microsystems, Germany).

Bright field immunostaining was performed for the localization of SOD2 protein in the hippocampus using Vectastain<sup>®</sup> ABC Kit (PK-6101, Vector Laboratories, CA, USA). Briefly,



**Fig. 2** rMTBI induces oxidative stress and downregulation of SOD2 in the hippocampus over 30 days. **a** ROS levels were estimated using H2DCFDA oxidation assay in the sham control (SC,  $n = 5$ ) and rMTBI-exposed rats at 48 h (5M-48h,  $n = 5$ ) and 30 days (5M-30d,  $n = 6$ ). **b** The oxidative DNA damage in the hippocampus was detected by 8-OHG immunofluorescence staining. Pictomicrographs showing the 8-OHG-positive cells in the subfields of hippocampus (CA1, CA2, CA3, and DG) of SC ( $n = 5$ ), 5M-48h ( $n = 5$ ), and 5M-30d ( $n = 5$ ) rats. Scale bar: 100  $\mu\text{m}$ . **c** The intensity was quantified and represented as percentage immunoreactive area in all the groups. **d** Degenerating neurons were detected by FJC staining. Pictomicrographs demonstrate the FJC-positive cells in CA3 and DG subfields of hippocampus in SC ( $n = 5$ ), 5M-48h ( $n = 5$ ), and 5M-30d ( $n = 5$ ) rats. Scale bar: 100  $\mu\text{m}$ . **e** The intensity of FJC-positive cells was quantified and represented as percentage immunoreactive area. **f** The mRNA levels and **g** protein (total and mitochondria) levels of SOD2 in the hippocampus of the sham ( $n = 5$ ) and rMTBI-exposed rats (5M-48h,  $n = 5$ ; 5M-30d,  $n = 5$ ). The blot images represent intensity of SOD2 protein expressed in SC, 5M-48h and 5M-30d rats. Quantitative analysis of protein levels was performed by intensity measurement of SOD2 with respect to  $\beta$ -actin (total) and HSP60 (mitochondrial). **h** The SOD2-positive cells were detected in the hippocampus of SC ( $n = 5$ ), 5M-48h ( $n = 5$ ), and 5M-30d ( $n = 5$ ) rats using immunolabeling. Pictomicrographs illustrate the SOD2 expression in the CA3 and DG regions at 48 h and 30 days post rMTBI. Scale bar: 100  $\mu\text{m}$ . **i** The SOD2-positive cells were quantified and represented as percentage immunoreactive area. **j** The overall SOD2 activity in the hippocampus was estimated in SC ( $n = 5$ ), 5M-48h ( $n = 5$ ), and 5M-30d ( $n = 5$ ) rats and represented as percentage of control. Values in the graphical representations are means ( $\pm$ SEM) and are indicated as significantly different as compared to controls ( $*p < 0.05$ ,  $**p < 0.01$ ,  $***p < 0.001$ ; one-way ANOVA followed by post hoc Tukey's test). The SOD2 function increased after 48 h of rMTBI and then alleviated at persistent time point. The details of statistical analyses are presented in Supplementary Table S2. ROS, reactive oxygen species; H2DCFDA, 2', 7'-dichlorodihydrofluorescein diacetate; SOD2, superoxide dismutase 2; rMTBI, repeated mild traumatic brain injury; 8-OHG, 8-hydroxyguanine; FJC, Fluoro Jade C; CA, cornu ammonis; DG, dentate gyrus

the sections were washed in PBS and treated with 0.3% hydrogen peroxide for 2 min. Sections were incubated with normal goat serum for 30 min followed by incubation in SOD2 rabbit polyclonal antibody (1:500 dilution; 06–984, Millipore, USA) overnight at 4 °C. Furthermore, the sections were washed and incubated with biotinylated goat anti-rabbit IgG antibodies at room temperature for 1 h (1:200). After washing, the sections were treated with ABC reagent (1:100) for 1 h followed by development of color using 3,3-diaminobenzidine tetrahydrochloride (DAB) as chromogen containing 0.02% H<sub>2</sub>O<sub>2</sub> for 8–10 min. Sections were washed in distilled water for 5 min, dehydrated and cleared in xylene for 15 min, and mounted on glass slides using DPX mountant (Merck, India). For all the SOD2 and 8-OHG immunostaining analyses, three images from each bregma-matched section from five sections of each animal (total 15 images from each animal) were subjected to morphometric analysis using Image J 1.45 software. The results were analyzed and represented as the mean percentage immunoreactive area ( $\pm$  SEM).

## Fluoro Jade C Staining

Fluoro Jade C (FJC) is a polyanionic fluorescein derivative which selectively binds to degenerating neurons [49]. The dye was applied to examine the dying neurons in the hippocampus of the animals exposed to rMTBI. For the detection of the degenerating neurons, the brain sections were mounted on gelatin-coated slides, air-dried, and subjected to FJC staining. In brief, the slides were rehydrated in absolute ethanol for 3 min and 70% ethanol for 1 min. The slides were incubated in 0.06% KMnO<sub>4</sub> solution for 15 min to reduce the background and prevent from photobleaching or fading. The FJC (AG325, Merck Millipore, USA) stock solution (0.01%) was prepared by dissolving in the distilled water. The appropriate working solution was achieved by making 0.001% FJC solution with glacial acetic acid. The slides were washed for 1 min and incubated with 0.001% FJC staining solution in the dark for 30 min. After 3 washes, the slide was air-dried, xylene cleared, and mounted with DPX mountant. The FITC filter was used for visualizing FJC staining on the epifluorescence microscope (DM-4500, Leica Microsystems, Germany). Three images from each bregma-matched section from five sections of each animal were subjected to morphometric analysis using Image J 1.45 software. The results are represented as the mean percentage reactive area ( $\pm$  SEM).

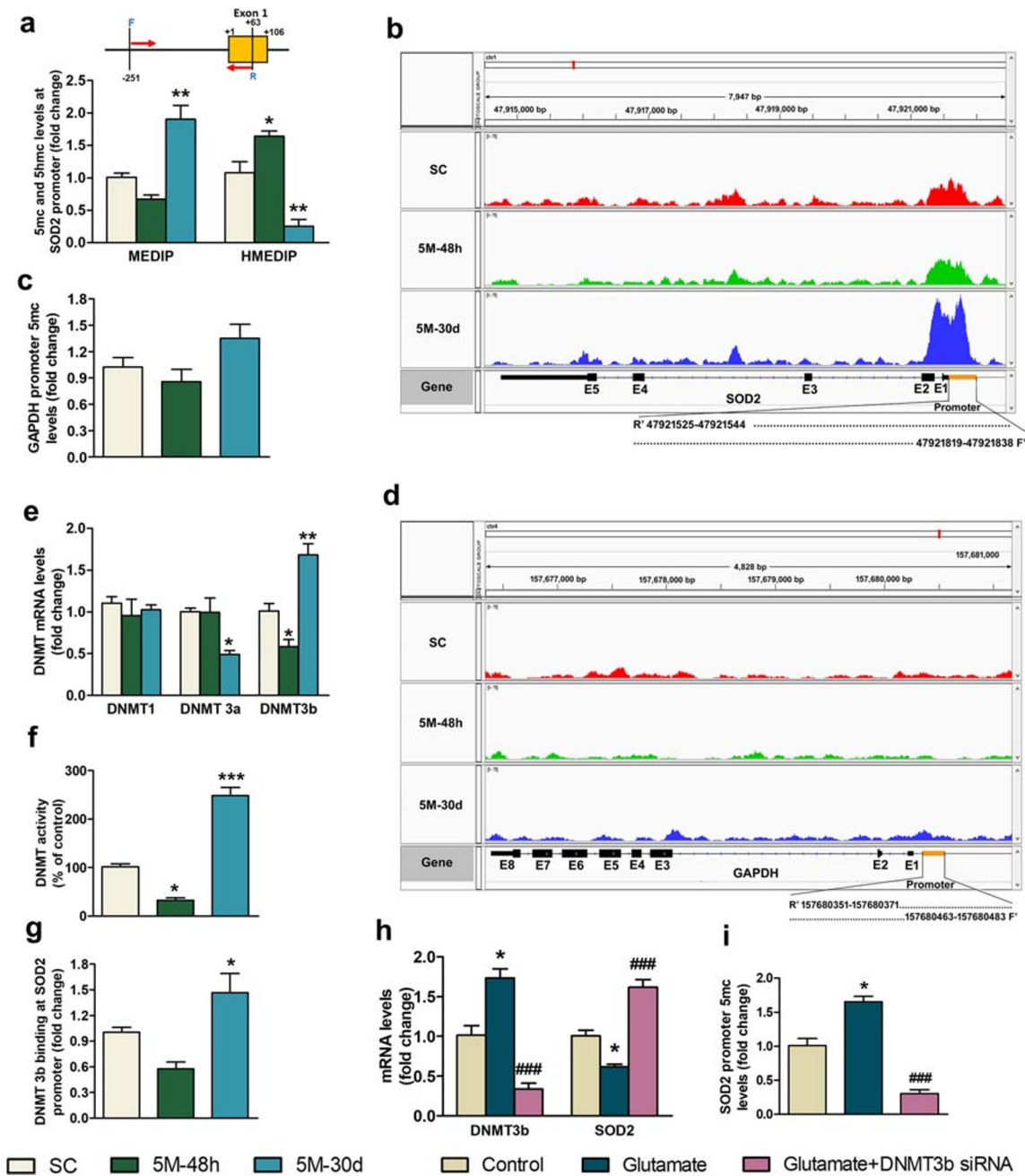
## Statistical Analyses

The differences among the groups included in the study with one episode of rMTBI/sham procedure were tested for the significance using one-way analysis of variance (ANOVA). The differences among the groups treated with (1) two episodes of either sham or rMTBI procedures and (2) 5-AzaC or vehicle treatment were analyzed using two-way ANOVA. The analysis of SOD2 and ROS levels among different groups with 1 or 3 traumatic hits was evaluated by two-way ANOVA (Supplementary Fig. S2). Post hoc analyses for all the ANOVA comparisons were performed using the Tukey's multiple comparison test. The  $p$  values less than 0.05 ( $p < 0.05$ ) were considered significant for all the analyses. All the statistical details for ANOVA analyses ( $F$  values,  $p$ -values, and  $df$  values) are provided in Supplementary Tables S1–S6.

## Results

### rMTBI-Induced Oxidative Stress and Neurodegenerative Changes

We have investigated the effects of single MTBI or rMTBI induced by 3 (3M) or 5 hits (5M) on total cellular ROS levels



in the hippocampus post 48 h and 30 days. The ROS levels were increased at 48 h ( $p < 0.05$ ) after exposure to 5 hits (5M-48h), which persisted until 30 days (5M-30d;  $p < 0.01$ ; Fig. 2a). However, the single MTBI or rMTBI by 3 hits could not provoke the ROS levels at both the time points (Supplementary Fig. S2a).

In order to examine the oxidative damage induced by rMTBI, we have measured the levels of 8-OHG, a DNA oxidation marker [26, 50]. The number of 8-OHG-positive cells were higher in all the sub-regions of the hippocampus [cornu ammonis (CA) 1, 2, 3 and dentate gyrus (DG)] at 48 h ( $p < 0.01$ ), while at 30 days, the maximum DNA damage was observed in the CA3 and DG ( $p < 0.01$ ; Fig. 2b, c).

Furthermore, the FJC staining was performed to quantify the number of degenerating neurons in the hippocampus. The number of FJC-positive degenerating neurons was higher in the CA3 region at both the time points ( $p < 0.01$  at 48 h and  $p < 0.001$  at 30 days), whereas number of such neurons was increased in the DG only at 30 days post rMTBI ( $p < 0.01$ ; Fig. 2d, e).

### rMTBI Caused SOD2 Dysfunction

The effects of rMTBI on functional expression of SOD2 in the hippocampus were tested by measuring its mRNA, protein, and activity levels at 48 h and 30 days after 5 hits (5M-48h and

◀ **Fig. 3** rMTBI induces persistent hypermethylation on SOD2 promoter via DNMT3b. **a** Quantification of 5mc (MeDIP) and 5hmc (HMeDIP) levels at SOD2 promoter of sham control (SC,  $n = 5$ ) and rMTBI-exposed rats (5M-48h,  $n = 5$  and 5M-30d,  $n = 6$ ). The line diagram illustrates the primers designed at SOD2 promoter for the qPCR analysis. **b** Integrated Genome Browser (IGB) view of 5mc peaks in SOD2 gene generated by MACS2 peak caller. Read coverage is represented in red (SC,  $n = 2$ ), green (5M-48h,  $n = 2$ ), and blue (5M-30d,  $n = 2$ ). Location of the SOD2 promoter primers used for MeDIP-qPCR is depicted below the gene track. **c** Quantification of 5mc levels at GAPDH promoter using MeDIP-qPCR in SC ( $n = 5$ ), 5M-48h ( $n = 5$ ), and 5M-30d ( $n = 6$ ) rats. **d** IGB view of 5mc peaks in GAPDH gene generated by MACS2 peak caller. Read coverage is represented in red (SC,  $n = 2$ ), green (5M-48h,  $n = 2$ ), and blue (5M-30d,  $n = 2$ ). **e** Relative quantification of mRNA levels of DNMT1, 3a and 3b isoforms in SC ( $n = 5$ ), 5M-48h ( $n = 5$ ), and 5M-30d ( $n = 5$ ) rats. **f** DNMT activity in SC ( $n = 5$ ), 5M-48h ( $n = 5$ ), and 5M-30d ( $n = 6$ ) rats. **g** Quantification of DNMT3b binding at SOD2 promoter using ChIP-qPCR in SC ( $n = 5$ ), 5M-48h ( $n = 5$ ), and 5M-30d ( $n = 6$ ) rats. The DNMT3b occupancy at the SOD2 promoter decreased at early time point and increased at 30 days post trauma which in turn increased DNA methylation and SOD2 repression. **h** The mRNA levels of SOD2 and DNMT3b. **i** 5mc levels in the SOD2 promoter in the untreated ( $n = 3$ ), glutamate only ( $n = 3$ ), and glutamate with DNMT3b siRNA-treated ( $n = 3$ ) PC12 cells. Values in the graphical representations are means ( $\pm$ SEM) and are indicated as significantly different as compared to sham control or untreated PC12 cells ( $*p < 0.05$ ,  $**p < 0.01$ ,  $***p < 0.001$ ; one-way ANOVA followed by post hoc Tukey's test); glutamate with DNMT3b siRNA-treated PC12 cells was also compared with glutamate only-treated cells ( $^{###}p < 0.001$ ; one-way ANOVA followed by post hoc Tukey's test). The results of statistical analyses are presented in Supplementary Table S3. 5mc, 5-methyl cytosine; 5hmc, 5-hydroxymethyl cytosine levels; SOD2, superoxide dismutase 2; GAPDH, glyceraldehyde 3-phosphate dehydrogenase; MeDIP, methylated DNA immunoprecipitation; IGB, Integrated Genome Browser; DNMT, DNA methyltransferase; ChIP, Chromatin immunoprecipitation; PC12, pheochromocytoma-12 cell-line; rMTBI, repeated mild traumatic brain injury

5M-30d). SOD2 mRNA and protein levels in whole hippocampal lysate, as measured by RT-qPCR and western blot respectively, were elevated at 48 h ( $p < 0.05$ ) after rMTBI but declined at 30 days ( $p < 0.01$ ; Fig. 2f, g). The changes in SOD2 protein levels in whole cell lysate were similar to that of the mitochondrial protein fractions, whereas SOD2 protein levels were increased at 48 h ( $p < 0.01$ ) and reciprocally decreased at 30 days ( $p < 0.01$ ; Fig. 2g). In addition, the immunohistochemical analyses of the hippocampus showed the similar changes as observed by western blot. The percentage of SOD2 immunoreactive area in the CA3 and DG subfields of hippocampus was heightened at 48 h ( $p < 0.01$ ), which was reciprocally waned at 30 days ( $p < 0.05$ ; Fig. 2h, i). Similar to the protein levels, the SOD2 activity was also augmented at 48 h after rMTBI ( $p < 0.05$ ) but declined at 30 days ( $p < 0.05$ ; Fig. 2j). In addition, we have also examined the mRNA levels of SOD2 in the hippocampus of rats exposed to single MTBI or rMTBI by 3 hits. On one hand, single MTBI did not alter SOD2 mRNA levels at both the time points; on the other hand, 3 hits increased the SOD2 levels at 48 h ( $p < 0.05$ ) which were subsequently normalized by 30 days (Supplementary Fig.

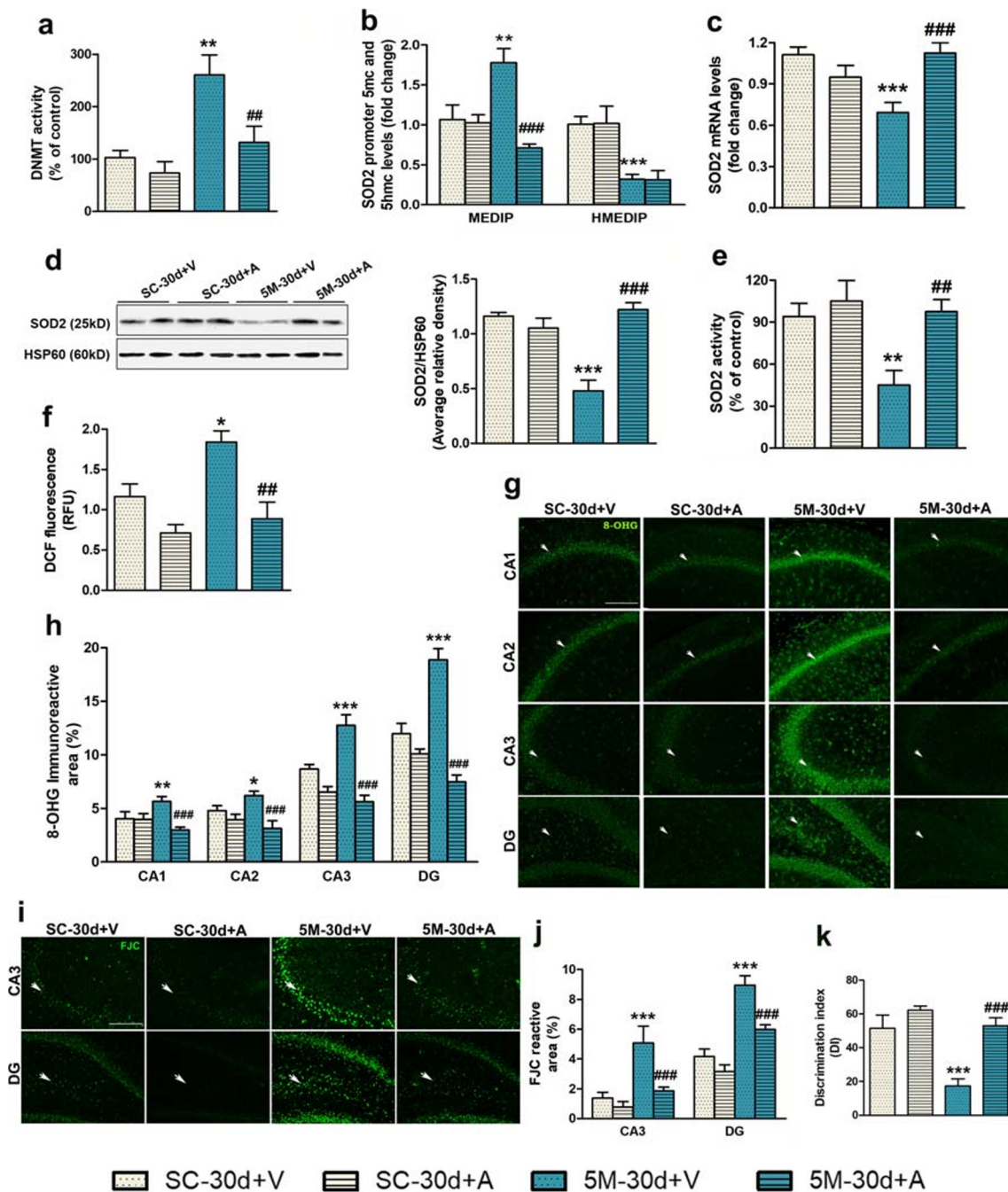
S2b). These results suggest that rMTBI induced by 5 hits, and not by 3 hits, is able to cause long-lasting changes in SOD2 functions via neuroadaptation.

In addition, we have also examined the catalase activity in the hippocampus post 48 h and 30 days of rMTBI. The catalase activity was increased at 48 h ( $p < 0.05$ ) which was further normalized by 30 days of rMTBI (Supplementary Fig. S3).

### rMTBI Silenced SOD2 Function via DNMT3b-Dependent DNA Methylation

The levels of cytosine methylation (5mc) and hydroxymethylation (5hmc) at the SOD2 promoter were examined using MeDIP-qPCR, HMeDIP-qPCR, and MeDIP-SEQ peak analysis. The MeDIP-qPCR analysis showed decreasing trend of 5mc levels ( $p < 0.184$ ) at SOD2 promoter (+63 to -251) after 48 h (Fig. 3a). On the contrary, significant hypermethylation was observed at 30 days of rMTBI ( $p < 0.01$ ; Fig. 3a). The MeDIP-SEQ peak analysis confirmed the observations from MeDIP-qPCR analysis. The methylation peak profile at the SOD2 locus verified the hypermethylation at the promoter region at the 30<sup>th</sup> day time point (Fig. 3b). The primer designed for MeDIP-qPCR spans the same promoter region of SOD2 gene that showed the hypermethylation in MeDIP-SEQ peak analysis (Fig. 3b). As opposed to the 5mc levels, the 5hmc levels were significantly elevated at 48 h ( $p < 0.05$ ) and declined at 30 days ( $p < 0.01$ ; Fig. 3a), which suggest the sequential effects of rMTBI on demethylation and methylation process at SOD2 promoter. As a control, the DNA methylation was also examined at the GAPDH promoter. The rMTBI did not alter the 5mc levels at GAPDH promoter as examined by both the MeDIP-qPCR (Fig. 3c) and MeDIP-SEQ peak analysis (Fig. 3d). These results indicate (i) the gene-specific effects of rMTBI and (ii) that the DNA methylation in SOD2 promoter was the result of rMTBI.

The effects of rMTBI on DNMTs were analyzed by measuring mRNA and protein activity levels in the hippocampus. The DNMT3a mRNA levels were reduced at 30 days ( $p < 0.05$ ). However, DNMT3b mRNA levels were reduced at 48 h ( $p < 0.05$ ) and increased at 30 days ( $p < 0.01$ ). DNMT1 mRNA levels were not affected by the rMTBI (Fig. 3e). As similar to the changes in DNMT3b mRNA levels, the DNMT activity was attenuated at 48 h ( $p < 0.05$ ) and was reciprocally enhanced at 30 days ( $p < 0.001$ ; Fig. 3f). As DNMT activity as well as DNMT3b mRNA levels was accentuated at 30 days, we have further investigated whether DNMT3b may be causal to SOD2 promoter methylation and thereby regulates its expression. The ChIP-qPCR analysis confirmed the occupancy of SOD2 promoter by DNMT3b. In parallel with the MeDIP analysis, the DNMT3b occupancy at SOD2 promoter was lowered at 48 h ( $p < 0.087$ ) with subsequent increase by 30 days ( $p < 0.05$ ; Fig. 3g).



The role of DNMT3b in the SOD2 promoter methylation and expression was further tested in vitro using DNMT3b-siRNA treatments to neurons derived from PC12 cells. To mimic the rMTBI-induced chronic oxidative stress conditions, cells were treated with sub-lethal dose of glutamate [38]. As expected, glutamate toxicity increased DNMT3b mRNA levels ( $p < 0.05$ ; Fig. 3h) which was coincident with 5mc levels at SOD2 promoter ( $p < 0.05$ ; Fig. 3i) and SOD2 mRNA levels ( $p < 0.05$ ; Fig. 3h). Moreover, the DNMT3b-siRNA transfection in the glutamate-treated cells reduced DNMT3b mRNA levels ( $p < 0.001$ ; Fig. 3h) with concomitant reduction in 5mc levels at SOD2 promoter ( $p < 0.001$ ; Fig. 3i)

thereby activating SOD2 expression ( $p < 0.001$ ; Fig. 3h). The in vitro as well as in vivo studies, therefore, suggest that the DNMT3b-dependent DNA methylation plays an important role in SOD2 expression, and the mechanism is dysregulated by rMTBI.

### 5-Azacytidine Revoked rMTBI-Induced Chronic Silencing of SOD2

From the above experiments, it seems reasonable to believe that the rMTBI induced long-lasting changes in DNA methylation at SOD2 promoter, likely via DNMT3b upregulation.

**Fig. 4** 5-Azacytidine restores rMTBI-induced DNMT3b-mediated SOD2 function and oxidative stress in the hippocampus. **a** Effect of 5-AzaC or vehicle treatment on DNMT activity. **b** 5mc and 5hmc levels at SOD2 promoter. **c** SOD2 mRNA levels in the hippocampus of sham control [SC-30d + V, ( $n = 5$ ); SC-30d + A, ( $n = 5$ )] and rMTBI-exposed rats [5M-30d + V ( $n = 5$ ); 5M-30d + A ( $n = 5$ –6)]. **d** The blot represents mitochondrial SOD2 levels in the hippocampus of SC-30d + V ( $n = 5$ ), 5M-30d + V ( $n = 5$ ), SC-30d + A ( $n = 5$ ), and 5M-30d + A ( $n = 5$ ) rats. The SOD2 protein quantification is represented as average relative density with respect to HSP60. **e** SOD2 activity in the hippocampus of SC-30d + V ( $n = 5$ ), 5M-30d + V ( $n = 5$ ), SC-30d + A ( $n = 5$ ), and 5M-30d + A ( $n = 5$ ) rats is represented as percentage of control. The treatment of 5-AzaC reversed the DNMT3b-induced DNA methylation at SOD2 promoter, thereby restoring its function. Effect of 5-AzaC or vehicle treatment on **f** ROS levels as measured by DCF fluorescence intensity and **g** DNA damage as measured by 8-OHG immunostaining in the hippocampus of sham control [SC-30d + V, ( $n = 5$ ); SC-30d + A, ( $n = 5$ )] and rMTBI-exposed rats [5M-30d + V ( $n = 5$ ); 5M-30d + A ( $n = 5$ )]. The pictomicrographs represent immunostaining of 8-OHG in the subfields of the hippocampus (CA1, CA2, CA3, and DG) of vehicle and 5-AzaC-treated sham control and rMTBI-exposed rats. Scale bar: 100  $\mu\text{m}$ . **h** 8-OHG-positive cells were quantified and represented as percentage immunoreactive area. **i** Degenerative neurons were measured by FJC staining. The pictomicrographs represent FJC-positive cells in subfields of hippocampus of sham control [SC-30d + V, ( $n = 5$ ); SC-30d + A, ( $n = 5$ )] and rMTBI-exposed rats [5M-30d + V ( $n = 5$ ); 5M-30d + A ( $n = 5$ )]. Scale bar: 100  $\mu\text{m}$ . **j** The FJC-positive cells were quantified and represented as percentage reactive area. 5-AzaC restored the rMTBI-induced SOD2 activity and thereby DNA damage and degenerating neurons in the hippocampus. **k** The effect of 5-AzaC or vehicle on discrimination index (DI) in the novel object recognition (NOR) test performed by SC-30d + V ( $n = 5$ ), 5M-30d + V ( $n = 5$ ), SC-30d + A ( $n = 5$ ), 5M-30d + A ( $n = 5$ ) rats. 5 AzaC treatment improved rMTBI-induced persistent deficits in learning and memory. Values in the graphical representations are means ( $\pm$ SEM) and are indicated as significantly different as compared to SC-30d + V (\* $p < 0.05$ , \*\* $p < 0.01$ , \*\*\* $p < 0.001$ ) and as compared to 5M-30d + V (## $p < 0.01$ , ### $p < 0.001$ ; two-way ANOVA followed by post hoc Tukey's test). The details of statistical analyses are presented in Supplementary Table S4. DNMT, DNA methyltransferase; ROS, reactive oxygen species; H2DCFDA, 2', 7'-dichlorodihydrofluorescein diacetate; SOD2, superoxide dismutase 2; rMTBI, repeated mild traumatic brain injury; 8-OHG, 8-hydroxyguanine; FJC, Fluoro Jade C; CA, cornu ammonis; DG, dentate gyrus

To reveal this causality, 5-AzaC was intraperitoneally injected to the rMTBI-exposed rats. As mentioned above (“rMTBI Caused SOD2 Dysfunction” section; Fig. 2f–j and “rMTBI Silenced SOD2 Function via DNMT3b-Dependent DNA Methylation” section; Fig. 3a), we have again observed the increase in the DNMT activity ( $p < 0.01$ ; Fig. 4a) hypermethylation in SOD2 promoter ( $p < 0.01$ ; Fig. 4b), decrease in its mRNA ( $p < 0.001$ ; Fig. 4c) and protein levels ( $p < 0.001$ ; Fig. 4d), and dampening of SOD2 activity ( $p < 0.01$ ; Fig. 4e) in the rMTBI-exposed rats treated with vehicle (5M-30d + V), as compared to the vehicle-treated sham controls (SC-30d + V). The 5-AzaC treatment (5M-30d + A) normalized the rMTBI-induced DNMT activity ( $p < 0.01$ ; Fig. 4a) and SOD2 promoter hypermethylation ( $p < 0.001$ ; Fig. 4b). Interestingly, the restoration of SOD2 promoter methylation by 5-AzaC

treatment concomitantly manifested in normalization of SOD2 mRNA ( $p < 0.001$ ; Fig. 4c), protein ( $p < 0.001$ ; Fig. 4d) and activity levels ( $p < 0.01$ ; Fig. 4e).

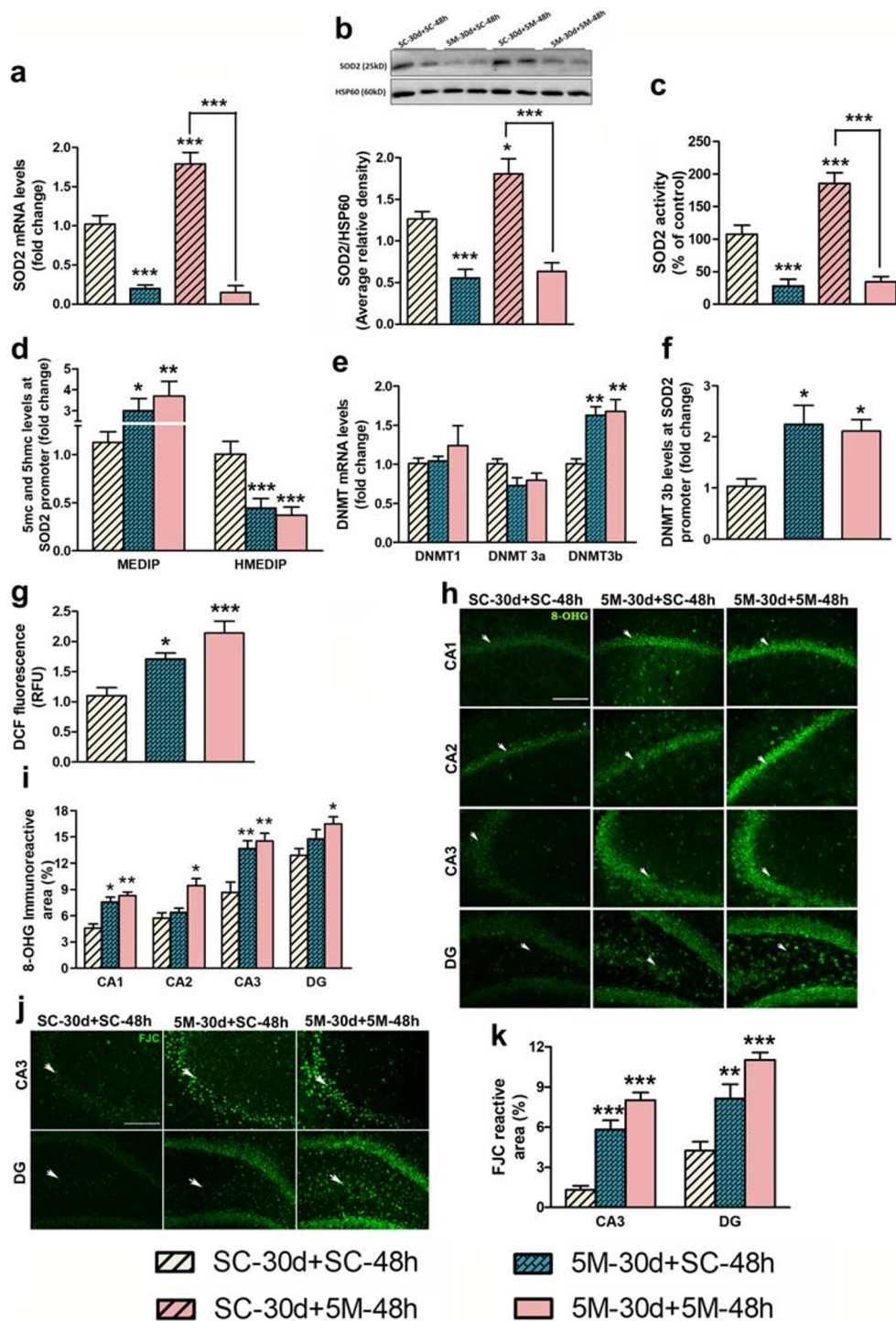
As observed previously (“rMTBI Silenced SOD2 Function via DNMT3b-Dependent DNA Methylation” section; Fig. 3a), the decrease in 5hmc levels at SOD2 promoter was observed in the vehicle-treated rMTBI-exposed rats, as compared to sham controls ( $p < 0.001$ ; Fig. 4b). However, the 5-AzaC treatment did not affect the hydroxymethylation, unlike DNA methylation (Fig. 4b). This emphasizes that the 5-AzaC was able to selectively decrease the DNA methylation without affecting the existing hydroxymethylation process at the SOD2 promoter.

### 5-Azacytidine Normalized rMTBI-Induced Oxidative Damage and Neurodegeneration

The above results emphasize the potential of 5-AzaC in restoring the SOD2 function via reversal of DNA hypermethylation at promoter. Hence, we hypothesized that the 5-AzaC treatment may restore the redox homeostasis in the hippocampus. To address this, the long-term oxidative stress levels were measured in the 5-AzaC-treated rats. Similar to the observations as mentioned in “rMTBI-Induced Oxidative Stress and Neurodegenerative Changes” section (Fig. 2a–c), the ROS levels and 8-OHG immunoreactivity were increased in the hippocampus of rMTBI-exposed rats treated with vehicle (5M-30d + V), as compared to that in the sham control rats (SC-30d + V) ( $p < 0.05$ , ROS, Fig. 4f and  $p < 0.01$ , CA1;  $p < 0.05$ , CA2;  $p < 0.001$ , CA3;  $p < 0.001$ , DG; 8-OHG, Fig. 4g, h). Furthermore, the elevated levels of ROS and 8-OHG immunoreactivity in rMTBI-exposed rats were restored by 5-AzaC treatment (5M-30d + A) compared to vehicle-treated rMTBI exposed rats (5M-30d + V;  $p < 0.01$ , ROS, Fig. 4f;  $p < 0.001$ , CA1, CA2, CA3, CA4, DG, 8-OHG, Fig. 4g, h).

As mentioned above (“rMTBI-Induced Oxidative Stress and Neurodegenerative Changes” section; Fig. 2d, e), the number of degenerating neurons, as measured by FJC staining, was higher in the CA3 ( $p < 0.001$ ) and DG ( $p < 0.001$ ) regions of hippocampus of rMTBI-exposed rats treated with vehicle (5M-30d + V), as compared to that in the vehicle-treated sham control rats (SC-30d + V; Fig. 4i, j). The question whether the DNA methylation-induced sequelae causing oxidative stress can lead to neurodegeneration was examined by 5-AzaC treatment. The number of FJC-positive cells was reduced in the CA3 ( $p < 0.001$ ) and DG ( $p < 0.001$ ) of rMTBI-exposed rats treated with 5-AzaC (5M-30d + A), as compared to that in the rMTBI-exposed rats treated with vehicle (5M-30d + V; Fig. 4i, j). However, the 5-AzaC treatment did not affect the oxidative stress indicators and the number of degenerating neurons in the sham controls (Fig. 4f–j).

We have previously reported that the rMTBI induce deficits in learning and memory as measured by NOR test [13].



The rMTBI-exposed rats treated with vehicle or 5-AzaC were subjected to the NOR test and DI was calculated as a measure of learning and memory. Similar to our previous reports, the DI was lower in the rMTBI-exposed rats (5M-30d + V) versus sham control rats (SC-30d + V;  $p < 0.001$ ; Fig. 4k). Furthermore, the DI in the rMTBI-exposed rats was improved by the treatment of 5-AzaC (5M-30d + A;  $p < 0.001$ ; Fig. 4k). However, 5-AzaC did not affect the DI in the sham controls (Fig. 4k). These results implicate the rMTBI-induced

DNMT3b-dependent SOD2 dysregulation as a crucial mechanism for inducing oxidative stress and neuropathology, which can be reversed by DNMT inhibitor treatment.

### Enduring Epigenetic Blockade of SOD2 Increased Susceptibility to the Second Episode of rMTBI

The above results pinpoint that the SOD2 gene is silenced by DNA methylation, which was able to chronically disrupt

**Fig. 5** Epigenetic silencing of SOD2 causes vulnerability to subsequent episodes of rMTBI. Graphs represent the **a** SOD2 mRNA levels, **b** mitochondrial SOD2 protein levels, and **c** SOD2 activity in the hippocampus of the rats exposed to single or double episode of rMTBI or sham procedures (SC-30d + SC-48h,  $n = 5$ ; 5M-30d + SC-48h,  $n = 5-6$ ; SC-30d + 5M-48h  $n = 5$ ; 5M-30d + 5M-48h  $n = 6$ ). The graph represents **d** 5mc and 5hmc levels at SOD2 promoter, **e** DNMT1, 3a, 3b mRNA levels, **f** DNMT3b occupancy at SOD2 promoter in the hippocampus of SC-30d + SC-48h ( $n = 5$ ), 5M-30d + SC-48h ( $n = 5-6$ ), and 5M-30d + 5M-48h ( $n = 6$ ) rats. **g** ROS levels as measured by DCF fluorescence intensity ( $n = 5$ ). **h** The pictomicrographs represent 8-OHG-positive cells in the subfields of the hippocampus (CA1, CA2, CA3, and DG) of SC-30d + SC-48h ( $n = 5$ ), 5M-30d + SC-48h ( $n = 5-6$ ), and 5M-30d + 5M-48h ( $n = 6$ ) rats. Scale bar: 100  $\mu\text{m}$ . **i** 8-OHG intensity were quantified and represented as percentage immunoreactive area. **j** The pictomicrographs represent FJC-positive cells in the CA3 and DG regions of the hippocampus of SC-30d + SC-48h ( $n = 5$ ), 5M-30d + SC-48h ( $n = 5-6$ ), and 5M-30d + 5M-48h ( $n = 6$ ) rats. Scale bar: 100  $\mu\text{m}$ . **k** Quantification of FJC reaction was represented as percentage immunoreactive area. The mean ( $\pm$ SEM) values for SOD2 mRNA, protein, and activity are significantly different as compared to SC-30d + SC-48h and SC-30d + 5M-48h ( $*p < 0.05$ ,  $***p < 0.001$ ; two-way ANOVA followed by post hoc Tukey's multiple comparisons test). The mean ( $\pm$ SEM) values for other molecular and biochemical experiments were performed by one-way ANOVA followed by post hoc Tukey's multiple comparisons test and the significant differences as compared to control (SC-30d + SC-48h) are indicated as  $*p < 0.05$ ,  $**p < 0.01$ ,  $***p < 0.001$ . SOD2 dysfunction was persistent even after exposure to double episode of rMTBI. The details of statistical analyses are presented in Supplementary Table S5. DNMT, DNA methyltransferase; ROS, reactive oxygen species; H2DCFDA, 2', 7'-dichlorodihydrofluorescein diacetate; SOD2, superoxide dismutase 2; rMTBI, repeated mild traumatic brain injury; 8-OHG, 8-hydroxyguanine; FJC, Fluoro Jade C; CA, cornu ammonis; DG, Dentate gyrus

redox homeostasis after rMTBI. Therefore, question arises whether the rMTBI-induced long-term repression of SOD2 can be revoked immediately after exposure to another episode of rMTBI, similar to that after the first episode. To address this, rats were exposed to single (5M-30d + SC-48h, SC-30d + 5M-48h) and double episodes of rMTBI (5M-30d + 5M-48h) and SOD2 function was measured in the hippocampus. The SOD2 mRNA, protein, and activity levels were declined in the rMTBI-exposed rats subjected to sham procedure during the second episode (5M-30d + SC-48h), as compared to double sham-exposed controls (SC-30d + SC-48h) ( $p < 0.001$ , SOD2 mRNA, protein, and activity; Fig. 5a–c). It may be recalled that the exposure to single episode of rMTBI elicited SOD2 function after 48 h (5M-48h; “rMTBI Caused SOD2 Dysfunction” section; Fig. 2f–j). Similarly, the SOD2 mRNA, protein, and activity levels of the sham-exposed rats were augmented after 48 h of the second rMTBI exposure (SC-30d + 5M-48h) compared to double sham-exposed controls (SC-30d + SC-48h;  $p < 0.001$ , mRNA and activity;  $p < 0.05$ , protein; Fig. 5a–c). On the contrary, SOD2 levels of the rats exposed to rMTBI during first episode were declined at 48 h after the second rMTBI exposure (5M-30d + 5M-48h) compared to sham-treated animals

exposed to rMTBI during the second episode (SC-30d + 5M-48h;  $p < 0.001$ , mRNA, protein, and activity; Fig. 5a–c). These findings revealed that the blockade created by DNA methylation at the SOD2 promoter after the first traumatic event culminated into permanent repression of SOD2 by 30 days, thus attenuating its response to additional episode of rMTBI. The MeDIP-qPCR was performed to investigate the DNA methylation at the SOD2 promoter in the rats subjected to the second episode of rMTBI. The SOD2 promoter was hypermethylated in sham- (5M-30d + SC-48h;  $p < 0.05$ ) and rMTBI-exposed rats (5M-30d + 5M-48h;  $p < 0.01$ ) during the second episode as compared to double sham-exposed rats (Fig. 5d). It is noted that the 5mc levels were maintained at higher levels even after 48 h of the second episode of rMTBI, unlike to what was observed after first episode of rMTBI (Fig. 3a). Concurrently, the 5hmc levels at the SOD2 promoter were significantly reduced ( $p < 0.001$ ) in both the groups (Fig. 5d).

We have further examined the involvement of DNMT3b in the persistent blockade of SOD2 expression via DNA methylation. DNMT3b mRNA levels were increased in rMTBI exposed rats (5M-30d + SC-48h;  $p < 0.01$ ), which were consistent after the second exposure to rMTBI (5M-30d + 5M-48h;  $p < 0.01$ ; Fig. 5e). Similarly, DNMT3b occupancy at the SOD2 promoter was increased in the rats exposed to single (5M-30d + SC-48h;  $p < 0.05$ ) and double episodes (5M-30d + 5M-48h;  $p < 0.05$ ) of rMTBI, as compared to double sham-exposed rats (Fig. 5f). The results after the second episode were opposite to what was observed at 48 h of the first episode of rMTBI (5M-48h; “rMTBI Silenced SOD2 Function via DNMT3b-Dependent DNA Methylation” section; Fig. 3e, g). The mRNA levels of other DNMT isoforms (DNMT1 and 3a) were not altered by the exposure to two episodes of rMTBI.

## Two Episodes of rMTBI-Enhanced Oxidative Stress and Neurodegeneration

The above results suggest that the exposure to repeated episode of rMTBI could not revoke the SOD2 function, as observed immediately after the first episode. As mentioned above (“rMTBI-Induced Oxidative Stress and Neurodegenerative Changes” and “rMTBI Caused SOD2 Dysfunction” sections; Fig. 2), the ROS levels were high in parallel with increased SOD2 function after 48 h of the first traumatic event. On the contrary, the SOD2 function was persistently dampened with reciprocal increase in ROS levels after 48 h of second sham/rMTBI exposure (5M-30d + SC-48h;  $p < 0.05$ ; 5M-30d + 5M-48h;  $p < 0.001$ ; Fig. 5g). Both, the 8-OHG and the FJC-reactive area were significantly increased in the rMTBI-exposed rats after 48 h of sham procedure (5M-30d + SC-48h) [ $p < 0.05$ , CA1;  $p < 0.01$ , CA3; 8-OHG, Fig. 5h, i) and ( $p < 0.001$ , CA3;  $p < 0.01$ , DG; FJC staining, Fig. 5j, k)] or rMTBI

procedure during the second episode (5M-30d + 5M-48h) [ $p < 0.01$ , CA1;  $p < 0.05$ , CA2;  $p < 0.01$ , CA3;  $p < 0.05$ , DG; 8-OHG, Fig. 5h, i) and ( $p < 0.001$ , CA3 and DG; FJC staining, Fig. 5j, k)] compared to double sham-exposed controls (SC-30d + SC-48h; Fig. 5h–k). These results suggest that the rMTBI-induced epigenetic blockade of SOD2 is causal to the increased susceptibility towards the damage from the subsequent injuries.

### Prophylactic Treatment of 5-azacytidine Relieved the Blockade in SOD2 Expression During Episodic rMTBI

The epigenetic blockade installed by DNA methylation at SOD2 promoter during the course of time after first traumatic event was able to maintain the suppression of SOD2 function after the second episode. Therefore, we hypothesized that erasing the DNA methylation induced by the first episode of rMTBI may help improve the SOD2 function after the second episode. To address this, we have intraperitoneally injected 5-AzaC post 30 days of the first episode of rMTBI/sham exposure and subjected these rats to the second episode. The 5mc levels were augmented in the rats which underwent single episode of rMTBI followed by sham treatment (5M-30d + V + SC-48h,  $p < 0.001$ ) and double episode of rMTBI (5M-30d + V + 5M-48h,  $p < 0.001$ ) as compared to rats exposed to sham treatment during both the episodes (SC-30d + V + SC-48h). Furthermore, the 5-AzaC treatment restored the rMTBI-induced DNA methylation (5M-30d + A + SC-48h) compared to rMTBI-exposed vehicle-treated rats (5M-30d + V + SC-48h,  $p < 0.001$ ). Therefore, the prophylactic treatment of 5-AzaC further reduced the 5mc levels at 48h after the second episode of rMTBI (5M-30d + A + 5M-48h), as compared to vehicle-treated rMTBI exposed rats (5M-30d + V + 5M-48h;  $p < 0.001$ ; Fig. 6a). On the contrary, the rats devoid of prophylactic treatment of 5-AzaC (5M-30d + V + 5M-48h) failed to restore the methylation status during the second episode, similar to that observed at 48 h after sham treatment of the rats subjected to the first episode of rMTBI (5M-30d + V + SC-48h; Fig. 6a).

We further examined whether the disruption of DNA methylation at SOD2 promoter by prophylactic treatment of 5-AzaC can improve the SOD2 response during the following event of rMTBI. The levels of SOD2 mRNA, protein, and activity were compromised after the single episode of rMTBI (5M-30d + V + SC-48h) compared to vehicle-treated sham exposed rats during both the episodes (SC-30d + V + SC-48h;  $p < 0.001$ , mRNA and activity;  $p < 0.01$ , protein; Fig. 6b–d) as similar to that explained in the “rMTBI Caused SOD2 Dysfunction” section and Fig. 2f–j. The 5-AzaC treatment after 30 days of the first rMTBI exposure normalized the SOD2 function after 48 h of the second episode of sham procedure (5M-30d + A + SC-48h) as compared to rMTBI-

exposed animals treated with vehicle and exposed to sham procedure during the second episode (5M-30d + V + SC-48h;  $p < 0.001$ , mRNA and protein;  $p < 0.01$ , activity). Therefore, the prophylactic treatment of 5-AzaC increased the SOD2 expression and activity after 48 h of the second episode of rMTBI (5M-30d + A + 5M-48h), as compared to double rMTBI-exposed vehicle-treated rats (5M-30d + V + 5M-48h;  $p < 0.001$ , mRNA, protein, and activity; Fig. 6b–d) and 5M-30d + A + SC-48h ( $p < 0.001$ , mRNA, protein, and activity). Similar to the methylation levels, the SOD2 expression during the second episode was not elicited in the rMTBI-exposed rats devoid of prophylactic treatment of 5-AzaC (5M-30d + V + 5M-48h), like observed in single rMTBI-exposed rats (5M-30d + V + SC-48h). These results suggest the prophylactic role of 5-AzaC to reinstate the DNA methylation status at the SOD2 promoter and rescue the rMTBI-induced chronic repression of SOD2 function.

### Discussion

The novel results of the present study demonstrate that (i) the DNA methylation by DNMT3b at SOD2 promoter regulates its expression in the hippocampus, (ii) rMTBI-induced DNA methylation causes persistent blockade of SOD2 function, and (iii) that DNMT inhibition is sufficient to restore the rMTBI-induced SOD2 dysfunction, cellular damage, and deficits in learning and memory. Although previous studies emphasized the role of SOD2-linked oxidative homeostasis in neurological disorders [32, 51], to our knowledge, the current study for the first time demonstrates the epigenetic blockade in SOD2 expression responsible for the long-lasting secondary injuries inflicted by repeated episodes of trauma.

Unlike SOD2 activation at acute phase of the first episode of rMTBI, the methylation at SOD2 promoter induced by the first episode obstructed SOD2 gene activation in response to second traumatic event. The notion that the SOD2 function is blocked by methylated promoter is supported by the fact that the changes in DNMT3b occupancy at SOD2 promoter parallel to DNA methylation levels and SOD2 function at different time points after the first and second episodes of rMTBI. Furthermore, the blockade of SOD2 expression is released by the therapeutic action of 5-AzaC in vivo and by the treatment of DNMT3b siRNA in vitro. Furthermore, the recovery of SOD2 function after 5-AzaC treatment was coincident with the reduction in rMTBI-induced neurodegenerative changes. It can be therefore emphasized that the rMTBI-induced DNA methylation at SOD2 promoter increases susceptibility to neural damage during the subsequent episodes. Taken together, these findings demonstrate the significant role of epigenetic blockade of SOD2 gene via DNMT3b-induced DNA methylation in neuroadaptive processes after rMTBI (Fig. 7).



TBI-induced glutamate excitotoxicity results into surge in ROS levels in different parts of the brain, such as hippocampus [52], cortex [53], and striatum [54]. Glutamate excitotoxicity increases intracellular  $\text{Ca}^{2+}$  levels through ionotropic receptors (NMDA and AMPA) and disrupts mitochondrial electron transport thereby producing excessive ROS [55]. Our results also show the similar surge in ROS levels at an acute time point post rMTBI. It is interesting to note that the ROS functions as a catalyst of DNA methylation and can induce site-specific hypermethylation via upregulation of

DNMT expression or by facilitating the formation of large complexes containing DNMT [56, 57].

The low dose of glutamate (5 mM) is known to increase global DNA methylation via alterations in DNMTs in the astrocyte-neuronal-endothelial co-culture system [58]. Similarly, in current study, the glutamate treatment (15 mM) to PC12 cell-derived neuronal cells upregulated DNMT3b expression coincident with the hypermethylation at SOD2 promoter. In line with this, we have also observed upregulation in DNMT function, particularly DNMT3b, in the

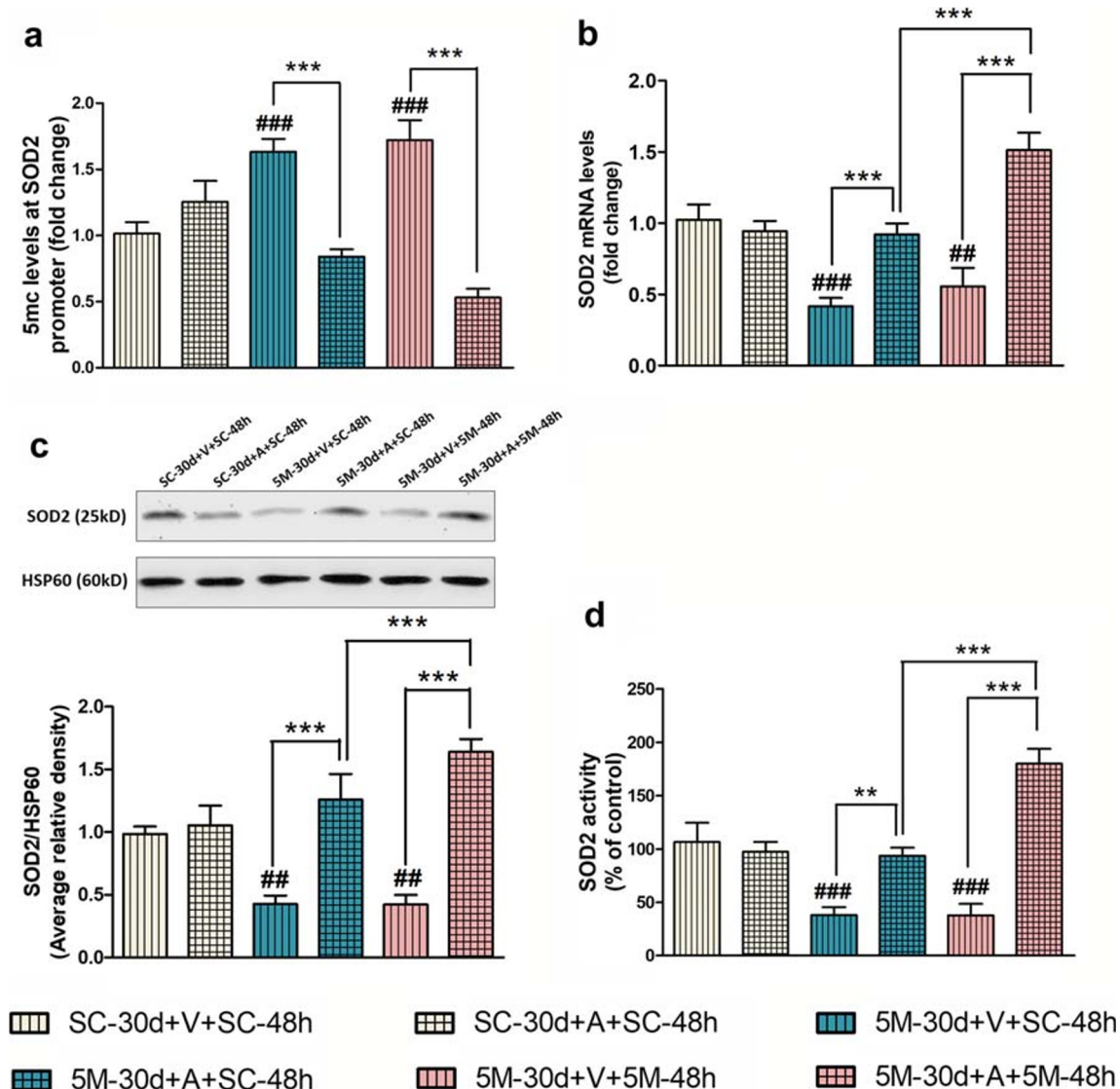


**Fig. 6** Prophylactic treatment of DNMT inhibitor (5-azacytidine) removed the rMTBI-induced epigenetic blockade at SOD2 promoter. Graphs showing **a** 5mC levels at SOD2 promoter, **b** SOD2 mRNA levels, **c** SOD2 protein levels, and **d** SOD2 activity in the hippocampus of sham controls treated with vehicle (SC-30d + V + SC-48h,  $n = 5$ ) or 5-AzaC (SC-30d + A + SC-48h,  $n = 5$ ), rMTBI-induced rats either treated with vehicle (5M-30d + V + SC-48h,  $n = 5$ ) or 5-AzaC (5M-30d + A + SC-48h,  $n = 5$ ) and double episodic rMTBI-exposed rats prophylactically treated with vehicle (5M-30d + V + 5M-48h,  $n = 5$ ) or 5-AzaC (5M-

30d + A + 5M-48h,  $n = 5$ ). The SOD2 function was restored after the prophylactic administration of 5-AzaC. Values in the graphical representations are means ( $\pm$ SEM) and are indicated as significantly different from SC-30d + V + SC-48h ( $##p < 0.01$ ,  $###p < 0.001$ ) and other groups ( $**p < 0.01$ ,  $***p < 0.001$ ). The statistical test was performed by using two-way ANOVA followed by post hoc Tukey's multiple comparisons test. The details of statistical analyses are presented in Supplementary Table S6. SOD2, superoxide dismutase 2; rMTBI, repeated mild traumatic brain injury; 5-AzaC, 5-azacytidine

hippocampus at protracted time point (30 days) post rMTBI; however, at early time point (48 h), DNMT activity and DNMT3b levels were decreased. Likewise, upregulation in the DNMT3b mRNA was reported in the hippocampus of the rats exposed to blast injury after 14 days [59]. In yet another model of MTBI, an air blast overpressure, global DNA hypermethylation is observed in the neurons of the frontal cortex post 8 months [37]. However, TBI induced by contusion, global DNA hypomethylation is reported after 1–2 days post injury [60]. Therefore, it may be speculated that the local glutamate toxicity accumulates over the course of time post TBI or rMTBI and elevates the levels of DNMT function and alter the DNA methylation dynamics at specific loci of the genome.

The rMTBI induced SOD2 promoter hypomethylation post 48 h, whereas hypermethylation post 30 days of injury. Reciprocally, the hydroxymethylation levels on the SOD2 promoter were increased at 48 h and decreased at 30 days. These results demonstrate the shift in dynamic equilibrium between demethylation and methylation status on the SOD2 promoter in the hippocampus at different time points after rMTBI. Similar observations were also reported in the

hippocampus of 8-month-old TgXFAD mice (Alzheimer's disease model) wherein global increase in 5mc was coincident with reciprocal decrease in 5hmc levels [61]. On the contrary, CpG methylation at Intron1 and not the promoter of SOD2 was also concomitant with the low levels of SOD2 expression and activity in the adrenal medulla of the P40 rats subjected to neonatal intermittent hypoxia [62]. Hence, it is noteworthy that any repeated exposure to stress paradigm such as rMTBI or intermittent hypoxia causes DNA hypermethylation at SOD2 promoter or Intron1.

SOD2 is reported to be crucial in the redox management in TBI pathology; however, the underlying mechanisms of its regulation are not known. In agreement with SOD2 promoter hypermethylation, high levels of DNMT3b were observed at chronic time point post rMTBI. The results of ChIP-qPCR show that the occupancy of DNMT3b at SOD2 promoter was associated with methylation levels and therefore further reaffirms the role of DNMT3b in SOD2 gene expression in the hippocampus. This mechanism was also validated in vitro (PC12 cell line derived neurons) using the glutamate toxicity to mimic rMTBI-induced oxidative stress. The DNMT3b siRNA could diminish the glutamate toxicity-induced

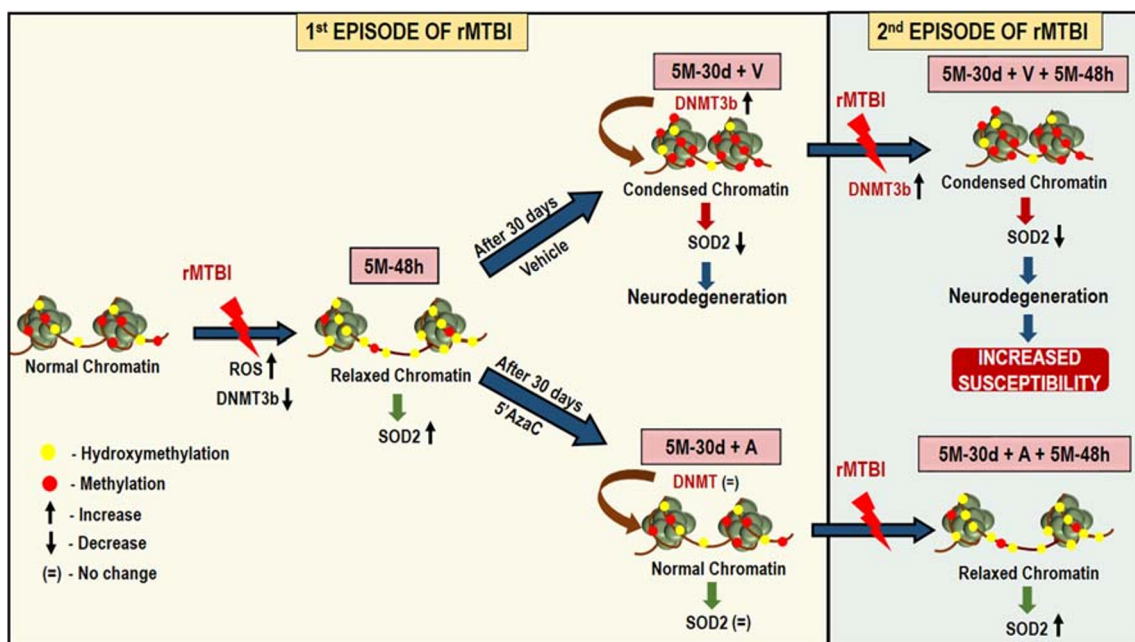


**Fig. 7** Schematic overview of the possible role of DNMT3b-mediated DNA methylation in the regulation of SOD2 during repeated episodes of rMTBI. The present study suggest that the rMTBI decreases the methylation (5mc) with concomitant increase in hydroxymethylation (5hmc) at SOD2 promoter by reducing the DNMT3b function at 48 h. During the course of time by 30 days, the neuroadaptation triggers the DNMT3b function at SOD2 promoter thereby causing the hypermethylation and reduction in SOD2 expression. The attenuated SOD2 function fails to contain the long-term oxidative damage precipitating into increased number of degenerating neurons. This blockade in SOD2 expression due to DNA methylation restricts the response to the second episode further worsening the consequences of the rMTBI such as neurodegeneration.

However, the DNMT inhibitor (5-AzaC) normalizes the methylation (5mc) at the SOD2 promoter thereby reducing the oxidative damage and the number of degenerative neurons. Moreover, the restoration of the promoter methylation by 5-AzaC allows the SOD2 activation in response to the second episode of rMTBI. Therefore, it may be inferred that the DNMT3b-regulated SOD2 function is causal to the rMTBI-induced oxidative damage and increased susceptibility to subsequent injuries which can be rescued by using DNMT inhibitors. rMTBI, repeated mild traumatic brain injury; DNMT3b, DNA methyltransferase 3b; ROS, reactive oxygen species; SOD2, superoxide dismutase 2; 5'AzaC, 5'azacytidine

hypermethylation at SOD2 promoter and also resume the SOD2 levels. Therefore, the results from *in vivo* as well as *in vitro* experiments endorse the causal role of DNMT3b in the SOD2 gene regulation post rMTBI via DNA methylation.

MTBI-induced gene-specific DNA hypermethylation represses gene expression, e.g., aralkylamine N-acetyltransferase (Aanat) gene [37]. Similarly, DNMT3b-mediated hypermethylation at SOD2 promoter repressed its expression at 30 days post rMTBI (5 hits); however, dramatic increase in SOD2 mRNA protein was observed at acute time point. Although previous studies using mild blast injury [34] and cortical stab injury (CSI) [63] support our results at an acute time point, observations at chronic time point differ. Huber and colleagues reported normalization of SOD2 expression in the hippocampus after 30 days of single mild blast injury [34]. We have observed no change in the SOD2 expression at acute and chronic time point after single mild injury, whereas after repeated (3 hits) mild injury, an increase of SOD2 levels at 48 h was observed with normalization at 30 days. The SOD2 expression pattern after single mild blast injury is coincident with 3 hits repeated mild injury of the current study, but not with 5 hits repeated mild injury paradigm. These discrepancies could be attributed to the exposure to single invasive injury [34] versus non-invasive, repeated mild traumatic events (current study). Moreover, the dynamic restorative process that occurs after single MTBI likely reduces the effects of glutamate toxicity over time [64]. On the contrary, the effects of the cumulative damage with each trauma of rMTBI are persistent over time and analogous to TBI [65, 66]. Therefore, the alleviated SOD2 levels in the hippocampus at 4 days post-unilateral cortical impact injury [52] and at 10 days post-CSI [63] can be supported by our observation about further temporal reduction of SOD2 at 30 days of rMTBI (current study). Hence, we may suggest that the mild but repetitive traumatic events undertake the persistent neuroadaptive changes in the SOD2 expression, and this neuroadaptation can be explained by promoter DNA hypermethylation. In addition, catalase activity was found to be increased at an acute time point, which was subsided by 30 days. The increase in the SOD2 and catalase activity post 48 h after rMTBI suggests the immediate response of antioxidant defense system against elevated ROS. Although catalase activity restored to normal levels, the SOD2 activity further declined by 30 days, precipitating into weak defense against accumulating ROS in hippocampus. Moreover, the oxidative stress triggered by TBI in the brain of SOD2 heterozygous knockout mice was rescued with overexpression of SOD2 [32]. Noteworthy is that the SOD2 heterozygous mice also display glutamate excitotoxicity due to lower expression of glutamate transporter 1 (GLT-1) and glutamate-aspartate transporter (GLAST) [67]. Hence, we argue in favor of rMTBI-induced glutamate excitotoxicity as a causal reason for the SOD2 dysfunction via DNA hypermethylation, which

in turn lead to mismanagement of ROS and pile up the oxidative stress.

Glutamate excitotoxicity exacerbates ROS levels [55]. We have observed excess ROS at 30 days post rMTBI in the hippocampus. ROS causes mitochondrial impairment and subsequently releases death effectors leading to neurodegeneration [68–71]. The 2-fold increase in the number of degenerating neurons of the hippocampus post 30 days of rMTBI could be due to glutamate excitotoxicity-induced excessive ROS. Plethora of clinical evidences suggest that the patients with rMTBI and those who survive moderate to severe TBI are at increased risk of developing long-term neurodegenerating diseases such as dementia, Alzheimer's disease [72–75], and Parkinson's disease [76–79].

Trauma-induced SOD2 hypofunction causes glutamate excitotoxicity and elevates ROS levels, thereby leading to neurodegeneration. Hippocampal neurodegeneration is widely associated with cognitive dysfunction [80–84]. Moreover, SOD2 heterozygous mice exhibit spatial memory impairment [26]. We have previously reported impairment in the learning and memory behavior assessed by NOR in the rats exposed to rMTBI [13]. Preclinical evidences reported mild TBI-induced hippocampal memory impairments such as deficits in learning and memory [15, 85], relative memory [86], and episodic memory [87]. With these evidences, we suggest that delayed but cumulative neuronal damage caused due to rMTBI-induced SOD2 hypofunction leads to learning and memory deficits.

To validate the involvement of DNMT in trauma-induced learning and memory deficits via SOD2, animals were treated with 5-AzaC, a pan DNMT inhibitor. The rMTBI-induced DNA hypermethylation and reduced SOD2 expression were restored after 5-AzaC treatment. Likewise, decitabine yet another inhibitor restored the DNA methylation and SOD2 levels in the adrenal medulla of the P40 rats exposed to neonatal intermittent hypoxia [62]. Previously, we have also reported the potential of 5-AzaC in restoring rMTBI-induced alterations in the BDNF gene expression and its promoter methylation in the amygdala [12]. The findings from our previous and current study suggest that 5-AzaC treatment ameliorates rMTBI-induced brain region-specific alterations in gene expressions. The treatment with 5-AzaC not only normalized the SOD2 activity, but also reversed the rMTBI-induced oxidative damage. To our knowledge, the results of the present study for the first time report the potential of DNMT inhibitor in controlling the oxidative damage in the brain, for which the underlying reason could be the restoration of SOD2 function. DNMT inhibitors including RG108, 5-AzaC, and zebularine are also reported as therapeutic drugs against various types of cancer cells [88–90]. The observations here appreciate their potential in treating oxidative stress-induced neurodegenerative disorders. A previous study by Endres and colleagues has reported lesions after ischemic

brain injury, which were reduced by 54% after 5-AzaC treatment [91]. Furthermore, in a recent study, intracerebroventricular injection of RG108 mitigated neurodegeneration and its behavioral correlates in a spinal and bulbar muscular atrophy [92]. In line with these studies, rMTBI-induced neurodegeneration-like phenotype was also ameliorated by 5-AzaC treatment by reinstating the SOD2 function. In addition, 5-AzaC treatment also reversed rMTBI-induced behavioral consequences such as anxiety-like behaviors [12] and deficits in learning and memory (current study). Perhaps, we may speculate that the restoration of SOD2 by DNMT inhibitor reinstated oxidative homeostasis thereby rescuing cellular and behavioral consequences of rMTBI. We may draw support from the previous studies wherein overexpression of SOD2 in the Alzheimer's disease- and TBI-exposed mice decreased hippocampal superoxide preventing learning and memory deficits [51] and cortical lesions [32], respectively. Moreover, the treatment with SOD mimetic drug, carboxyfullerene, improved learning and memory behaviors in aging mice [28]. Hence, the significance of DNMT3b-mediated DNA methylation at SOD2 promoter can be underscored in oxidative stress-induced deficits in learning and memory.

The epigenetic blockade of SOD2 gene during the first episode might lead to enhanced susceptibility to oxidative stress after second episode. Although the ROS was augmented by repeated episodes of rMTBI, the concurrent acute response by SOD2 was not observed. This could be explained by the hypermethylation at SOD2 promoter arresting its response to repeated episodes of rMTBI. The study highlights that the SOD2 dysfunction due to the first traumatic event exacerbates the susceptibility to recurring trauma. Therefore, intervention by DNMT inhibitor after initial traumatic events may shield against the oxidative damage during subsequent trauma.

It is significant to note that the females express high levels of endogenous antioxidant defense system as compared to males [93, 94]. Obviously, males are therefore assumed to be more susceptible to glutamate excitotoxicity [95] and TBI-induced oxidative stress [96]. This is also supported by a clinical study in more than 10,000 patients, wherein the recovery rates among women patients were better than in men suffering from mild to severe TBI [97]. Owing to the sexual differences in oxidative stress and defense mechanisms, the non-inclusion of female rats in the current study remains as a limitation. Therefore, future studies are warranted to understand the relevance of neuroadaptive SOD2 function in neurological effects of the brain trauma in females.

In sum, the present study suggests rMTBI-induced glutamate toxicity increases DNMT3b, which over time hypermethylates SOD2 promoter culminating into SOD2 hypofunction. Furthermore, SOD2 hypofunction exacerbated glutamate excitotoxicity accumulating excessive ROS, which causes neurodegeneration in the hippocampus. The mechanism is causal to deficits in the learning and memory behavior

post rMTBI. Hence, DNMT-induced persistent pro-oxidant state in hippocampus culminates into neurodegeneration and deficits in the learning and memory behavior (Fig. 7). These findings further advocate the therapeutic potential of DNMT inhibitors in treating oxidative stress-induced behavioral deficits.

**Acknowledgments** The authors kindly acknowledge Dr. Chaitanya Athale, Indian Institute of Science Education and Research-Pune (IISER-Pune), India, for the generous gift of PC12 cell line cultures and Institute for Applied Biological Research and Development (IABRD), Pune, for their technical support in *in vitro* experiments.

**Funding** This work was supported by the grants from the University Grants Commission, Government of India (UGC-GOI; F.4-5/151-FRP/2014/BSR); Science and Engineering Research Board (SERB), GOI (EMR/2017/000621); and Council for Scientific and Industrial Research (CSIR), GOI (37[1718]/18/EMR-II) to AJS. AJS also acknowledges funds received through the Department Research and Development Program of the Department of Biotechnology, Savitribai Phule Pune University, Pune, India. NB thanks the UGC-GOI for the award of Senior Research Fellowship (File No. 2061330923). SS acknowledges DST INSPIRE-Faculty program (DST/INSPIRE/04/2018/000529) for the funding support. DMK acknowledges the grants from the University Research Project Scheme (URPS; Dev./RTMNURP/AH/2115) from Rashtrasant Tukadoji Maharaj Nagpur University, Nagpur.

## Compliance with Ethical Standards

**Conflict of Interest** The authors declare that they have no conflict of interest.

**Ethical Approval** All applicable international, national, and institutional guidelines for the care and use of animals were followed.

## References

- Dewan MC, Rattani A, Gupta S, Baticulon RE, Hung YC, Panchak M, Agrawal A, Adeleye AO et al (2019) Estimating the global incidence of traumatic brain injury. *J Neurosurg* 130:1080–1097. <https://doi.org/10.3171/2017.10.JNS17352>
- Theadom A, Starkey NJ, Dowell T, Hume PA, Kahan M, McPherson K, Feigin V, BIONIC Research Group (2014) Sports-related brain injury in the general population: an epidemiological study. *J Sci Med Sport* 17:591–596. <https://doi.org/10.1016/j.jsams.2014.02.001>
- Manley G, Gardner AJ, Schneider KJ, Guskiewicz KM, Bailes J, Cantu RC, Castellani RJ, Turner M et al (2017) A systematic review of potential long-term effects of sport-related concussion. *Br J Sports Med* 51:969–977. <https://doi.org/10.1136/bjsports-2017-097791>
- Peskind ER, Brody D, Cernak I, McKee A, Ruff RL (2013) Military- and sports-related mild traumatic brain injury: clinical presentation, management, and long-term consequences. *J Clin Psychiatry* 74:180–188. <https://doi.org/10.4088/JCP.12011co1c>
- McKee AC, Robinson ME (2014) Military-related traumatic brain injury and neurodegeneration. *Alzheimers Dement* 10. <https://doi.org/10.1016/j.jalz.2014.04.003>
- Belanger HG, Spiegel E, Vanderploeg RD (2010) Neuropsychological performance following a history of multiple

- self-reported concussions: a meta-analysis. *J Int Neuropsychol Soc* 16:262–267. <https://doi.org/10.1017/S1355617709991287>
7. Combs HL, Berry DTR, Pape T, Babcock-Parziale J, Smith B, Schleenbaker R, Shandera-Ochsner A, Harp JP et al (2015) The effects of mild traumatic brain injury, post-traumatic stress disorder, and combined mild traumatic brain injury/post-traumatic stress disorder on returning veterans. *J Neurotrauma* 32:956–966. <https://doi.org/10.1089/neu.2014.3585>
  8. Vasterling JJ, Brailey K, Proctor SP, Kane R, Heeren T, Franz M (2012) Neuropsychological outcomes of mild traumatic brain injury, post-traumatic stress disorder and depression in Iraq-deployed US Army soldiers. *Br J Psychiatry* 201:186–192. <https://doi.org/10.1192/bjp.bp.111.096461>
  9. Ling H, Morris HR, Neal JW, Lees AJ, Hardy J, Holton JL, Revesz T, Williams DDR (2017) Mixed pathologies including chronic traumatic encephalopathy account for dementia in retired association football (soccer) players. *Acta Neuropathol* 133:337–352. <https://doi.org/10.1007/s00401-017-1680-3>
  10. Shively SB, Edgerton SL, Iacono D, Purohit DP, Qu BX, Haroutunian V, Davis KL, Diaz-Arrastia R et al (2017) Localized cortical chronic traumatic encephalopathy pathology after single, severe axonal injury in human brain. *Acta Neuropathol* 133:353–366. <https://doi.org/10.1007/s00401-016-1649-7>
  11. Shultz SR, Bao F, Omana V, Chiu C, Brown A, Cain DP (2012) Repeated mild lateral fluid percussion brain injury in the rat causes cumulative long-term behavioral impairments, neuroinflammation, and cortical loss in an animal model of repeated concussion. *J Neurotrauma* 29:281–294. <https://doi.org/10.1089/neu.2011.2123>
  12. Sagarkar S, Bhamburkar T, Shelkar G, Choudhary A, Kokare DM, Sakharkar AJ (2017) Minimal traumatic brain injury causes persistent changes in DNA methylation at BDNF gene promoters in rat amygdala: a possible role in anxiety-like behaviors. *Neurobiol Dis* 106:101–109. <https://doi.org/10.1016/j.nbd.2017.06.016>
  13. Sagarkar S, Balasubramanian N, Mishra S, Choudhary AG, Kokare DM, Sakharkar AJ (2019) Repeated mild traumatic brain injury causes persistent changes in histone deacetylase function in hippocampus: implications in learning and memory deficits in rats. *Brain Res* 1711:183–192. <https://doi.org/10.1016/j.brainres.2019.01.022>
  14. Prins ML, Alexander D, Giza CC, Hovda DA (2013) Repeated mild traumatic brain injury: mechanisms of cerebral vulnerability. *J Neurotrauma* 30:30–38. <https://doi.org/10.1089/neu.2012.2399>
  15. Aungst SL, Kabadi SV, Thompson SM, Stoica BA, Faden AI (2014) Repeated mild traumatic brain injury causes chronic neuroinflammation, changes in hippocampal synaptic plasticity, and associated cognitive deficits. *J Cereb Blood Flow Metab* 34:1223–1232. <https://doi.org/10.1038/jcbfm.2014.75>
  16. Luo J, Nguyen A, Villeda S, Zhang H, Ding Z, Lindsey D, Bieri G, Castellano JM et al (2014) Long-term cognitive impairments and pathological alterations in a mouse model of repetitive mild traumatic brain injury. *Front Neurol* 5:12. <https://doi.org/10.3389/fneur.2014.00012>
  17. Werner C, Engelhard K (2007) Pathophysiology of traumatic brain injury. *Br J Anaesth* 99:4–9. <https://doi.org/10.1093/bja/aem131>
  18. Bains M, Hall ED (2012) Antioxidant therapies in traumatic brain and spinal cord injury. *Biochim Biophys Acta Mol basis Dis* 1822: 675–684. <https://doi.org/10.1016/j.bbadis.2011.10.017>
  19. Cornelius C, Crupi R, Calabrese V, Graziano A, Milone P, Pennisi G, Radak Z, Calabrese EJ et al (2013) Traumatic brain injury: oxidative stress and neuroprotection. *Antioxid Redox Signal* 19: 836–853. <https://doi.org/10.1089/ars.2012.4981>
  20. Maas AI, Stocchetti N, Bullock R (2008) Moderate and severe traumatic brain injury in adults. *Lancet Neurol* 7:728–741. [https://doi.org/10.1016/S1474-4422\(08\)70164-9](https://doi.org/10.1016/S1474-4422(08)70164-9)
  21. Rodriguez-Rodriguez A, Egea-Guerrero J, Murillo-Cabezas F, Carrillo-Vico A (2014) Oxidative stress in traumatic brain injury. *Curr Med Chem* 21:1201–1211. <https://doi.org/10.2174/0929867321666131217153310>
  22. Arundine M, Tymianski M (2004) Molecular mechanisms of glutamate-dependent neurodegeneration in ischemia and traumatic brain injury. *Cell Mol Life Sci* 61:657–668. <https://doi.org/10.1007/s00018-003-3319-x>
  23. Abdul-Muneer PM, Chandra N, Haorah J (2015) Interactions of oxidative stress and neurovascular inflammation in the pathogenesis of traumatic brain injury. *Mol Neurobiol* 51:966–979. <https://doi.org/10.1007/s12035-014-8752-3>
  24. Singh IN, Sullivan PG, Deng Y, Mbye LH, Hall ED (2006) Time course of post-traumatic mitochondrial oxidative damage and dysfunction in a mouse model of focal traumatic brain injury: implications for neuroprotective therapy. *J Cereb Blood Flow Metab* 26: 1407–1418. <https://doi.org/10.1038/sj.jcbfm.9600297>
  25. Flynn JM, Melov N (2013) SOD2 in mitochondrial dysfunction and neurodegeneration. *Free Radic Biol Med* 62:4–12. <https://doi.org/10.1016/j.freeradbiomed.2013.05.027>
  26. Carvajal FJ, Mira RG, Rovegno M, Minniti AN, Cerpa W (2018) Age-related NMDA signaling alterations in SOD2 deficient mice. *Biochim Biophys Acta Mol basis Dis* 1864:2010–2020. <https://doi.org/10.1016/j.bbadis.2018.03.019>
  27. Oh SS, Sullivan KA, Wilkinson JE, Backus C, Hayes JM, Sakowski SA, Feldman EL (2012) Neurodegeneration and early lethality in superoxide dismutase 2-deficient mice: a comprehensive analysis of the central and peripheral nervous systems. *Neuroscience* 212:201–213. <https://doi.org/10.1016/j.neuroscience.2012.03.026>
  28. Quick KL, Ali SS, Arch R, Xiong C, Wozniak D, Dugan LL (2008) A carboxyfullerene SOD mimetic improves cognition and extends the lifespan of mice. *Neurobiol Aging* 29:117–128. <https://doi.org/10.1016/j.neurobiolaging.2006.09.014>
  29. Vincent AM, Russell JW, Sullivan KA, Backus C, Hayes JM, McLean LL, Feldman EL (2007) SOD2 protects neurons from injury in cell culture and animal models of diabetic neuropathy. *Exp Neurol* 208:216–227. <https://doi.org/10.1016/j.expneurol.2007.07.017>
  30. Namjoshi DR, Good C, Cheng WH, Panenka W, Richards D, Cripton PA, Wellington CL (2013) Towards clinical management of traumatic brain injury: a review of models and mechanisms from a biomechanical perspective. *Dis Model Mech* 6:1325–1338. <https://doi.org/10.1242/dmm.011320>
  31. Mychasiuk R, Farran A, Angoa-Perez M, Briggs D, Kuhn D, Esser MJ (2014) A novel model of mild traumatic brain injury for juvenile rats. *J Vis Exp* 94. <https://doi.org/10.3791/51820>
  32. Xiong Y, Shie FS, Zhang J, Lee CP, Ho YS (2005) Prevention of mitochondrial dysfunction in post-traumatic mouse brain by superoxide dismutase. *J Neurochem* 95:732–744. <https://doi.org/10.1111/j.1471-4159.2005.03412.x>
  33. Khatri N, Thakur M, Pareek V, Kumar S, Sharma S, Datusalia AK (2018) Oxidative stress: major threat in traumatic brain injury. *CNS Neurol Disord Drug Targets* 17:689–695. <https://doi.org/10.2174/1871527317666180627120501>
  34. Huber BR, Meabon JS, Martin TJ, Mourad PD, Bennett R, Kraemer BC, Cernak I, Petrie EC et al (2013) Blast exposure causes early and persistent aberrant phospho- and cleaved-tau expression in a murine model of mild blast-induced traumatic brain injury. *J Alzheimers Dis* 37:309–323. <https://doi.org/10.3233/JAD-130182>
  35. Kuehner JN, Bruggeman EC, Wen Z, Yao B (2019) Epigenetic regulations in neuropsychiatric disorders. *Front Genet* 10. <https://doi.org/10.3389/fgene.2019.00268>
  36. Stricker SH, Götz M (2018) DNA-methylation: master or slave of neural fate decisions? *Front Neurosci* 12:2018. <https://doi.org/10.3389/fnins.2018.00005.eCollection>
  37. Haghghi F, Ge Y, Chen S, Xin Y, Umali MU, de Gasperi R, Gama Sosa MA, Ahlers ST et al (2015) Neuronal DNA methylation

- profiling of blast-related traumatic brain injury. *J Neurotrauma* 32: 1200–1209. <https://doi.org/10.1089/neu.2014.3640>
38. Jia J, Zhang L, Shi X, Wu M, Zhou X, Liu X, Huo T (2016) SOD2 mediates amifostine-induced protection against glutamate in PC12 cells. *Oxidative Med Cell Longev* 2016. <https://doi.org/10.1155/2016/4202437>
  39. Bhamre AP, Borkar CD, Bodakuntla S, Lahiri M, Subhedar NK, Kokare DM (2016) Pro-cognitive action of CART is mediated via ERK in the hippocampus. *Hippocampus* 26:1313–1327. <https://doi.org/10.1002/hipo.22608>
  40. Ennaceur A, Delacour J (1988) A new one-trial test for neurobiological studies of memory in rats. 1: behavioral data. *Behav Brain Res* 31:47–59. [https://doi.org/10.1016/0166-4328\(88\)90157-X](https://doi.org/10.1016/0166-4328(88)90157-X)
  41. Burke SN, Wallace JL, Nematollahi S, Uprety AR, Barnes CA (2010) Pattern separation deficits may contribute to age-associated recognition impairments. *Behav Neurosci* 124:559–573. <https://doi.org/10.1037/a0020893>
  42. Aggleton JP, Albasser MM, Aggleton DJ, Poirier GL, Pearce JM (2010) Lesions of the rat perirhinal cortex spare the acquisition of a complex configural visual discrimination yet impair object recognition. *Behav Neurosci* 124:55–68. <https://doi.org/10.1037/a0018320>
  43. Oliveira AMM, Hawk JD, Abel T, Havekes R (2010) Post-training reversible inactivation of the hippocampus enhances novel object recognition memory. *Learn Mem* 17:155–160. <https://doi.org/10.1101/lm.1625310>
  44. Jaillard T, Roger M, Galinier A, Guillou P, Benani A, Leloup C, Casteilla L, Penicaud L et al (2009) Hypothalamic reactive oxygen species are required for insulin-induced food intake inhibition: an NADPH oxidase-dependent mechanism. *Diabetes* 58:1544–1549. <https://doi.org/10.2337/db08-1039>
  45. Sagarkar S, Mahajan S, Choudhary AG, Borkar CD, Kokare DM, Sakharkar AJ (2017) Traumatic stress-induced persistent changes in DNA methylation regulate neuropeptide Y expression in rat jejunum. *Neurogastroenterol Motil* 29. <https://doi.org/10.1111/nmo.13074>
  46. Balasubramanian N, Srivastava A, Pawar N, Sagarkar S, Sakharkar AJ (2019) Repeated mild traumatic brain injury induces persistent variations in mitochondrial DNA copy number in mesocorticolimbic neurocircuitry of the rat. *Neurosci Res* 155:34–42. <https://doi.org/10.1016/j.neures.2019.06.003>
  47. Schmittgen TD, Livak KJ (2008) Analyzing real-time PCR data by the comparative CT method. *Nat Protoc* 3:1101–1108. <https://doi.org/10.1038/nprot.2008.73>
  48. Thorvaldsdóttir H, Robinson JT, Mesirov JP (2013) Integrative genomics viewer (IGV): high-performance genomics data visualization and exploration. *Brief Bioinform* 14:178–192. <https://doi.org/10.1093/bib/bbs017>
  49. Ehara A, Ueda S (2009) Application of Fluoro-Jade C in acute and chronic neurodegeneration models: utilities and staining differences. *Acta Histochem Cytochem* 42:171–179. <https://doi.org/10.1267/ahc.09018>
  50. Lovell MA, Markesbery WR (2001) Ratio of 8-hydroxyguanine in intact DNA to free 8-hydroxyguanine is increased in Alzheimer disease ventricular cerebrospinal fluid. *Arch Neurol* 58:392–396. <https://doi.org/10.1001/archneur.58.3.392>
  51. Massaad CA, Washington TM, Pautler RG, Klann E (2009) Overexpression of SOD-2 reduces hippocampal superoxide and prevents memory deficits in a mouse model of Alzheimer's disease. *Proc Natl Acad Sci U S A* 106:13576–13581. <https://doi.org/10.1073/pnas.0902714106>
  52. Ansari MA, Roberts KN, Scheff SW (2008) Oxidative stress and modification of synaptic proteins in hippocampus after traumatic brain injury. *Free Radic Biol Med* 45:443–452. <https://doi.org/10.1016/j.freeradbiomed.2008.04.038>
  53. Yang LY, Greig NH, Tweedie D, Jung YJ, Chiang YH, Hoffer BJ, Miller JP, Chang KH et al (2020) The p53 inactivators pifithrin- $\mu$  and pifithrin- $\alpha$  mitigate TBI-induced neuronal damage through regulation of oxidative stress, neuroinflammation, autophagy and mitophagy. *Exp Neurol* 324. <https://doi.org/10.1016/j.expneurol.2019.113135>
  54. Huang YN, Yang LY, Greig NH, Wang YC, Lai CC, Wang JY (2018) Neuroprotective effects of pifithrin- $\alpha$  against traumatic brain injury in the striatum through suppression of neuroinflammation, oxidative stress, autophagy, and apoptosis. *Sci Rep* 8:2368. <https://doi.org/10.1038/s41598-018-19654-x>
  55. Krishnamurthy K, Laskowitz DT (2016) Cellular and molecular mechanisms of secondary neuronal injury following traumatic brain injury. In: *Translational Research in Traumatic Brain Injury*. pp. 97–126
  56. Weitzman SA, Turk PW, Milkowski DH, Kozlowski K (1994) Free radical adducts induce alterations in DNA cytosine methylation. *Proc Natl Acad Sci U S A* 91:1261–1264. <https://doi.org/10.1073/pnas.91.4.1261>
  57. Fan W, Luo J (2010) SIRT1 regulates UV-induced DNA repair through deacetylating XPA. *Mol Cell* 39:247–258. <https://doi.org/10.1016/j.molcel.2010.07.006>
  58. Zhao H, Sun P, Fan T, Yang X, Zheng T, Sun C (2019) The effect of glutamate-induced excitotoxicity on DNA methylation in astrocytes in a new in vitro neuron-astrocyte-endothelium co-culture system. *Biochem Biophys Res Commun* 508:1209–1214. <https://doi.org/10.1016/j.bbrc.2018.12.058>
  59. Bailey ZS, Grinter MB, De La Torre CD, VandeVord PJ (2015) Blast induced neurotrauma causes overpressure dependent changes to the DNA methylation equilibrium. *Neurosci Lett* 604:119–123. <https://doi.org/10.1016/j.neulet.2015.07.035>
  60. Zhang ZY, Zhang Z, Fauser U, Schluesener HJ (2007) Global hypomethylation defines a sub-population of reactive microglia/macrophages in experimental traumatic brain injury. *Neurosci Lett* 429:1–6. <https://doi.org/10.1016/j.neulet.2007.09.061>
  61. Griñán-Ferré C, Sarroca S, Ivanova A, Puigoriol-Illamola D, Aguado F, Camins A, Sanfeliu C, Pallàs M (2016) Epigenetic mechanisms underlying cognitive impairment and Alzheimer disease hallmarks in 5XFAD mice. *Aging (Albany NY)* 8:664–684. <https://doi.org/10.18632/aging.100906>
  62. Nanduri J, Makarenko V, Reddy VD, Yuan G, Pawar A, Wang N, Khan SA, Zhang X et al (2012) Epigenetic regulation of hypoxic sensing disrupts cardiorespiratory homeostasis. *Proc Natl Acad Sci U S A* 109:2515–2520. <https://doi.org/10.1073/pnas.1120600109>
  63. Parabucki AB, Božić ID, Bjelobaba IM, Lavrnja IC, Brkić PD, Jovanović TS, Savić DZ, Stojiljković MB et al (2012) Hyperbaric oxygenation alters temporal expression pattern of superoxide dismutase 2 after cortical stab injury in rats. *Croat Med J* 53:586–597. <https://doi.org/10.3325/cmj.2012.53.586>
  64. Iverson GL (2005) Outcome from mild traumatic brain injury. *Curr Opin Psychiatry* 18:301–317. <https://doi.org/10.1097/01.yco.0000165601.29047.ae>
  65. Barkhoudarian G, Hovda DA, Giza CC (2011) The molecular pathophysiology of concussive brain injury. *Clin Sports Med* 30:33–48. <https://doi.org/10.1016/j.csm.2010.09.001>
  66. Giza CC, Hovda DA (2014) The new neurometabolic cascade of concussion. *Neurosurgery* 75:S24–S33. <https://doi.org/10.1227/NEU.0000000000000505>
  67. Liang LP, Waldbaum S, Rowley S, Huang TT, Day BJ, Patel M (2012) Mitochondrial oxidative stress and epilepsy in SOD2 deficient mice: Attenuation by a lipophilic metalloporphyrin. *Neurobiol Dis* 45:1068–1076. <https://doi.org/10.1016/j.nbd.2011.12.025>
  68. Cowan K, Anichtchik O, Luo S (2019) Mitochondrial integrity in neurodegeneration. *CNS Neurosci Ther* 25:825–836

69. Zorov DB, Juhaszova M, Sollott SJ (2014) Mitochondrial reactive oxygen species (ROS) and ROS-induced ROS release. *Physiol Rev* 94:909–950
70. Redza-Dutordoir M, Averill-Bates DA (2016) Activation of apoptosis signalling pathways by reactive oxygen species. *Biochim Biophys Acta, Mol Cell Res* 1863:2977–2992. <https://doi.org/10.1016/j.bbamer.2016.09.012>
71. Marchi S, Giorgi C, Suski JM, Agnoletto C, Bononi A, Bonora M, de Marchi E, Missiroli S et al (2012) Mitochondria-Ros crosstalk in the control of cell death and aging. *J Signal Transduct* 2012:1–17. <https://doi.org/10.1155/2012/329635>
72. Schaffert J, LoBue C, White CL, Chiang HS, Didehban N, Lacritz L, Rossetti H, Dieppa M et al (2018) Traumatic brain injury history is associated with an earlier age of dementia onset in autopsy-confirmed Alzheimer's disease. *Neuropsychology* 32:410–416. <https://doi.org/10.1037/neu0000423>
73. Li Y, Li Y, Li X, Zhang S, Zhao J, Zhu X, Tian G (2017) Head injury as a risk factor for dementia and Alzheimer's disease: a systematic review and meta-analysis of 32 observational studies. *PLoS One* 12:e0169650. <https://doi.org/10.1371/journal.pone.0169650>
74. Abner EL, Nelson PT, Schmitt FA, Browning SR, Fardo DW, Wan L, Jicha GA, Cooper GE et al (2014) Self-reported head injury and risk of late-life impairment and AD pathology in an AD center cohort. *Dement Geriatr Cogn Disord* 37:294–306. <https://doi.org/10.1159/000355478>
75. Fleminger S, Oliver DL, Lovestone S, Rabe-Hesketh S, Giora A (2003) Head injury as a risk factor for Alzheimer's disease: the evidence 10 years on; a partial replication. *J Neurol Neurosurg Psychiatry* 74:857–862. <https://doi.org/10.1136/jnnp.74.7.857>
76. Gardner RC, Byers AL, Barnes DE, Li Y, Boscardin J, Yaffe K (2018) Mild TBI and risk of Parkinson disease: a chronic effects of neurotrauma consortium study. *Neurology* 90:E1771–E1779. <https://doi.org/10.1212/WNL.0000000000005522>
77. Raj R, Kaprio J, Korja M, Mikkonen ED, Jousilahti P, Siironen J (2017) Risk of hospitalization with neurodegenerative disease after moderate-to-severe traumatic brain injury in the working-age population: a retrospective cohort study using the Finnish national health registries. *PLoS Med* 14:e1002316. <https://doi.org/10.1371/journal.pmed.1002316>
78. Crane PK, Gibbons LE, Dams-O'Connor K, Trittschuh E, Leverenz JB, Keene CD, Sonnen J, Montine TJ et al (2016) Association of traumatic brain injury with late-life neurodegenerative conditions and neuropathologic findings. *JAMA Neurol* 73:1062–1069. <https://doi.org/10.1001/jamaneurol.2016.1948>
79. Jafari S, Etminan M, Aminzadeh F, Samii A (2013) Head injury and risk of Parkinson disease: a systematic review and meta-analysis. *Mov Disord* 28:1222–1229. <https://doi.org/10.1002/mds.25458>
80. Fernandes MYD, Carmo MRSD, Fonteles AA, Neves JCS, Silva ATAD, Pereira JF, Ferreira EO, Lima NMR et al (2019) (-)-A-Bisabolol prevents neuronal damage and memory deficits through reduction of proinflammatory markers induced by permanent focal cerebral ischemia in mice. *Eur J Pharmacol* 842:270–280. <https://doi.org/10.1016/j.ejphar.2018.09.036>
81. Nobili A, Latagliata EC, Viscomi MT, Cavallucci V, Cutuli D, Giacobuzzo G, Krashia P, Rizzo FR et al (2017) Dopamine neuronal loss contributes to memory and reward dysfunction in a model of Alzheimer's disease. *Nat Commun* 8. <https://doi.org/10.1038/ncomms14727>
82. Kotloski R, Lynch M, Lauersdorf S, Sutula T (2002) Repeated brief seizures induce progressive hippocampal neuron loss and memory deficits. In: *Progress in Brain Research*. pp. 95–110
83. Lee B, Sur B, Cho SG, Yeom M, Shim I, Lee H, Hahm DH (2016) Wogonin attenuates hippocampal neuronal loss and cognitive dysfunction in trimethyltin-intoxicated rats. *Biomol Ther* 24:328–337. <https://doi.org/10.4062/biomolther.2015.152>
84. Min D, Mao X, Wu K, Cao Y, Guo F, Zhu S, Xie N, Wang L et al (2012) Donepezil attenuates hippocampal neuronal damage and cognitive deficits after global cerebral ischemia in gerbils. *Neurosci Lett* 510:29–33. <https://doi.org/10.1016/j.neulet.2011.12.064>
85. Mouzon B, Chaytow H, Crynen G, Bachmeier C, Stewart J, Mullan M, Stewart W, Crawford F (2012) Repetitive mild traumatic brain injury in a mouse model produces learning and memory deficits accompanied by histological changes. *J Neurotrauma* 29:2761–2773. <https://doi.org/10.1089/neu.2012.2498>
86. Monti JM, Voss MW, Pence A, McAuley E, Kramer AF, Cohen NJ (2013) History of mild traumatic brain injury is associated with deficits in relational memory, reduced hippocampal volume, and less neural activity later in life. *Front Aging Neurosci* 5. <https://doi.org/10.3389/fnagi.2013.00041>
87. Yan H, Feng Y, Wang Q (2016) Altered effective connectivity of hippocampus-dependent episodic memory network in mTBI survivors. *Neural Plast* 2016:1–12. <https://doi.org/10.1155/2016/6353845>
88. Brueckner B, Boy RG, Siedlecki P, Musch T, Kliem HC, Zielenkiewicz P, Suhai S, Wiessler M (2005) Epigenetic reactivation of tumor suppressor genes by a novel small-molecule inhibitor of human DNA methyltransferases. *Cancer Res* 65:6305–6311. <https://doi.org/10.1158/0008-5472.CAN-04-2957>
89. Gayet O, Loncle C, Duconseil P, Gilabert M, Lopez MB, Moutardier V, Turrini O, Calvo E et al (2015) A subgroup of pancreatic adenocarcinoma is sensitive to the 5-aza-dC DNA methyltransferase inhibitor. *Oncotarget* 6:746–754. <https://doi.org/10.18632/oncotarget.2685>
90. Yang PM, Lin YT, Shun CT, Lin SH, Wei TT, Chuang SH, Wu MS, Chen CC (2013) Zebularine inhibits tumorigenesis and stemness of colorectal cancer via p53-dependent endoplasmic reticulum stress. *Sci Rep* 3. <https://doi.org/10.1038/srep03219>
91. Endres M, Meisel A, Biniszkiwicz D, Namura S, Prass K, Ruscher K, Lipski A, Jaenisch R et al (2000) DNA methyltransferase contributes to delayed ischemic brain injury. *J Neurosci* 20:3175–3181. <https://doi.org/10.1523/jneurosci.20-09-03175.2000>
92. Kondo N, Tohna G, Sahashi K, Iida M, Kataoka M, Nakatsuji H, Tsutsumi Y, Hashizume A et al (2019) DNA methylation inhibitor attenuates polyglutamine-induced neurodegeneration by regulating Hes5. *EMBO Mol Med* 11. <https://doi.org/10.15252/emmm.201708547>
93. Gaignard P, Fréchet M, Liere P, Théron P, Schumacher M, Slama A, Guennoun R (2018) Sex differences in brain mitochondrial metabolism: influence of endogenous steroids and stroke. *J Neuroendocrinol* 30. <https://doi.org/10.1111/jne.12497>
94. Khalifa ARM, Abdel-Rahman EA, Mahmoud AM, Ali MH, Noureldin M, Saber SH, Mohsen M, Ali SS (2017) Sex-specific differences in mitochondria biogenesis, morphology, respiratory function, and ROS homeostasis in young mouse heart and brain. *Physiol Rep* 5. <https://doi.org/10.14814/phy2.13125>
95. Demarest TG, McCarthy MM (2014) Sex differences in mitochondrial (dys)function: Implications for neuroprotection. *J Bioenerg Biomembr* 47:173–188
96. Rubin TG, Lipton ML (2019) Sex differences in animal models of traumatic brain injury. *J Exp Neurosci* 13:117906951984402. <https://doi.org/10.1177/1179069519844020>
97. Gupte R, Brooks W, Vukas R, Pierce J, Harris J (2019) Sex differences in traumatic brain injury: what we know and what we should know. *J Neurotrauma* 36:3063–3091